CONTRACT NO. A932-094
FINAL REPORT
APRIL 1998

Development and Application of an Up-To-Date Photochemical Mechanism for Airshed Modeling and Reactivity Assessment

CALIFORNIA ENVIRONMENTAL PROTECTION AGENCY

AIR RESOURCES BOARD
Research Division

DEVELOPMENT AND APPLICATION OF AN UP-TO-DATE PHOTOCHEMICAL MECHANISM FOR AIRSHED MODELING AND REACTIVITY ASSESSMENT

Final Report
Contract No. A932-094

Prepared for:

California Air Resources Board
Research Division
2020 L Street
Sacramento, CA 95814

Prepared by:

William P. L. Carter
Principal Investigator

Statewide Air Pollution Research Center
University of California
Riverside, CA 92521-0312

April 1998

For more information about the ARB's Research Division,
its research and activities, please visit our Web site:

http://www.arb.ca.gov/rd/rd.htm

ABSTRACT

The objective of this program is to address the research needs of California Air Resources Board (ARB) concerning the development and implementation of a state-of-the-art photochemical mechanism used in airshed models, and the application of these models for developing effective control strategies to reduce ozone. In response to the ARB's requests, the major focus of this program was the development of the Maximum Incremental Reactivity (MIR) scale which was implemented in the ARB's "Clean Fuels/Low-Emissions Vehicle" regulations as a means to calculate ozone reactivity adjustment factors (RAFs) so that volatile organic compound (VOC) emissions from different fuel/vehicle combinations can be regulated on an equal ozone impact basis. The main body of this report documents the development of the MIR and other reactivity scales, and discusses how best to develop an optimum scale for ozone reactivity assessment for VOCs. It is concluded that the MIR scale gives similar RAFs as a scale based on effects of VOCs on integrated ozone, and that either type of scale is appropriate for applications requiring use of a single reactivity scale.

Appendices to this report give the details of the chemical mechanism, airshed model scenarios, and calculation methodology employed, and give tabulations of results of selected sensitivity calculations on reactivity scales which were carried out. The latter include comparing reactivity scales developed in this work with those calculated using the two chemical mechanisms most commonly used in airshed models, and using a preliminary alternative aromatics mechanism which was developed for this program.

ACKNOWLEDGEMENTS

The author wishes to acknowledge the project officer for this program, Mr. Bart Croes of the Research Division of the ARB for his important contributions to the success of this project. His contributions went far beyond the normal duties of a project officer. He contributed substantially to the process of developing the reactivity scale, particularly regarding the establishment of the scenario conditions, and the implementation of the Lurmann, Carter and Coyner (LCC) mechanism. The author also acknowledges the contributions of the members of the ARB's Reactivity Advisory Panel (RAP) in the many discussions and meetings we had while the scale was developed. Most of the decisions concerning details of the scenario conditions were made in consultation with Mr. Croes and the members of the RAP and other scientists. The author also wishes to thank Mr. Keith Bauges for supplying the EKMA scenarios used in this study; Dr. Harvey Jeffries for supplying the actinic flux data used in these calculations, the computer files used to implement the Carbon Bond mechanism, and other useful data files and information; Dr. Michael Gery for providing the highly useful review of the chemical mechanism and helpful discussions; Dr. Roger Atkinson for helpful discussions concerning the chemical mechanism; and Mr. Alvin Lowi for initiating the project which ultimately led to the adoption of an incremental reactivity scale as a means to assess ozone impacts of vehicle emissions.

Although this work incorporates the contributions of Mr. Croes and the members of the RAP, the statements and conclusions in this report are entirely those of the author and not necessarily those of the California Air Resources Board. The mention of trade names and commercial products, their source or their use in connection with the material reported herein is not to be construed either an actual or implied endorsement of such products.

This report was submitted fulfillment of ARB Contract No. A934-094 under the sponsorship of the California Air Resources Board. Work was completed as of April 26, 1993.

TABLE OF CONTENTS

LIST OF TABLES

LIST OF FIGURES

INTRODUCTION

The formation of ground-level ozone is a serious air pollution problem in many urban areas. Ozone is not emitted directly, but is formed from the photochemical interactions of emitted volatile organic compounds (VOCs) and oxides of nitrogen (NO_x). To reduce ground level ozone levels and achieve existing air quality standards, it is necessary to reduce emissions of both of these ozone precursors. VOC controls reduce the rate at which ozone is formed and thus have the greatest effects on the concentrations of ozone nearer the source areas, while NO_x controls reduce the ultimate amount of ozone which can be formed, and thus have the greatest effects on ozone downwind of the source areas. Traditionally ozone control strategies have focused on VOC controls, though it is now clear that the ground-level ozone pollution problem will not be solved unless significant new NO_x controls are also implemented. However, is also clear that VOC control will continue to be an important part of any comprehensive ozone control strategy.

In developing cost-effective VOC control strategies for reducing ozone, it is important to recognize that not all VOCs affect ozone formation equally. These differences are referred to as the "reactivities" of the VOCs. Although in the past differences in VOC reactivities have often been neglected and all VOCs have been regulated equally, in recent years it has become recognized that control strategies designed to encourage the use of less reactive VOCs may provide a way to achieve ozone reductions which would not otherwise be cost-effective. An important example of this is use of alternative vehicle fuels. However, practical implementation of such strategies requires some means to quantify the reactivities of VOCs.

There are a number of ways to quantify VOC reactivities. Many previous reactivity scales are based on amounts of ozone formed when the VOC is irradiated in the presence of NO_x in environmental chambers (e.g., Wilson and Doyle, 1970; Altshuller and Bufalini, 1971; Laity et al., 1973). However, individual VOCs are almost never emitted the absence of other reactive organics, so such experiments do not represent atmospheric conditions. In addition, chamber effects are known to significantly affect results of such experiments (Bufalini et al., 1977; Joshi et al., 1982; Carter et al., 1982), particularly if the compound reacts relatively slowly or has radical sinks in its mechanism (Carter et al., 1986a; Carter and Lurmann, 1990, 1991). Because of this, single organic-NO_x-air experiments are not considered a reliable means for quantifying reactivity. An alternative measure of reactivity is the OH radical rate constant for the VOC (e.g., Darnall et al., 1976; CARB, 1989), since for most compounds this is the

main factor which determines its atmospheric lifetime (Atkinson, 1989, 1990). The advantages of this reactivity scale are that it is universal and that OH rate constants are known or can be estimated for most of the major types of VOCs which are emitted (Atkinson, 1987, 1989, 1990). However, it does not account for the significant differences in VOC reaction mechanisms (e.g., see Gery et al. 1988; Atkinson, 1989; Carter, 1990), which can affect how much ozone is formed once the VOC reacts (Carter and Atkinson, 1987, 1989a).

The most direct measure of ozone reactivity of a VOC is the change in ozone caused by changing the emissions of the VOC in an air pollution episode. This takes into account not only the effects of all aspects of the organic's reaction mechanism, but also effects of the environment where it is emitted. This can be estimated by computer airshed models, provided that the models have an adequate representation both of the conditions of the episode and of the kinetics and mechanisms of the VOC reactions that affect ozone formation. This approach has been employed in a number of modeling studies of the effects of VOC emission changes on ozone formation (e.g., Bufalini and Dodge, 1983; Dodge, 1984; Hough and Derwent, 1987; Carter and Atkinson, 1989a; Chang and Rudy, 1990), and it is the approach which is used in this work. Although the results are no more valid than the model of the chemical reactions or the air pollution episode being considered, modeling provides the potential for the most realistic and flexible means to assess the many factors which affect VOC reactivity and for the development of VOC reactivity scales.

The effect of changing the emissions of a given VOC on ozone formation in a particular episode will in general depend on the magnitude of the emission change and on whether the VOC is being added to, subtracted from, or replacing a portion of the base case (i.e., present day) emissions. However, for general reactivity assessment purposes, the amount added, subtracted, or substituted is essentially arbitrary. To avoid the dependence on this arbitrary parameter, we proposed use of "incremental reactivity" to quantify ozone impacts of VOCs (Carter and Atkinson, 1987,). This is defined as the change on ozone caused by adding an arbitrarily small amount of the test VOC to the emissions in the episode, divided by the amount of test VOC added. This can also be called the "local sensitivity" of ozone to the VOC, or the derivative of ozone with respect to emissions of the VOC.

$$\text{Incremental Reactivity of a VOC in an Episode} = \lim_{\text{VOC Added} \to 0} \left[\frac{\text{Ozone formed in the episode with the test VOC Added (Test Case)} - \text{Ozone formed in the episode (base case)}}{\text{Amount of VOC Added in the Test Case}} \right] \quad \text{(I)}$$

$$= \left. \frac{\partial [O_3]}{\partial [\text{test VOC}]} \right|_{NO_x, \text{ Other VOCs, Other scenario conditions}}$$

This approach also has the advantage that incremental reactivities of mixtures can be obtained by linear summation of the incremental reactivities of their components. This has obvious advantages in the assessment of reactivities of complex mixtures, such as vehicle exhausts (e.g., see Lowi and Carter, 1990, CARB, 1990).

Since incremental reactivities measure the effects of adding small amounts of VOCs, they do not necessarily predict the effects of large changes in emissions, as might occur, for example, if all the motor vehicles in an airshed were converted to another type of fuel. However, Chang and Rudy (1990) found that incremental reactivities give good approximations to effects on ozone of alternative fuel substitution scenarios involving changing 30% of the total VOC emissions. In any case, incremental reactivities will predict the direction of an initial ozone trend which results when a control strategy is phased in, and in most cases should also give a good approximation of the result once the control strategy is completely implemented.

Incremental reactivities of VOCs have been investigated in a number of computer modeling studies (Bufalini and Dodge, 1983; Dodge, 1984; Hough and Derwent, 1987; Carter 1989a, 1989b; Weir et al., 1988; Carter and Atkinson, 1989a; Chang and Rudy, 1990), and the VOC's reaction mechanism was found to be important in affecting its incremental reactivity. Some compounds can cause the formation of 10 or more additional molecules of ozone per carbon atom reacted, either directly or through its effects on reactions of other compounds, while others cause almost no ozone formation when they react, or even cause ozone formation to be reduced (e.g., see Carter and Atkinson, 1989a). The predictions that VOCs have variable effects on ozone formation, even after differences in reaction rates are taken into account, and that some have negative effects on ozone formation under some conditions, have been verified experimentally (e.g., Carter Atkinson, 1987).

The modeling studies also indicate that incremental reactivities of VOCs can depend significantly on the environmental conditions (e.g., Dodge, 1984; Carter and Atkinson, 1989a). The most important is the availability of NO_x, which is traditionally measured by the ratio of total emissions of reactive organic gases (ROG) to NO_x. In general, VOCs have the highest effects on ozone formation under relatively high NO_x conditions (i.e., low ROG/NO_x ratios) and to have much lower, in some cases even negative, reactivities under conditions where NO_x is limited (high ROG/NO_x ratios). This is because under relatively high NO_x conditions the amount of ozone formed is determined by the levels of radicals formed from the reactions of the VOCs, while under lower NO_x conditions it is the availability of NO_x, which must be present in order for ozone to be formed, which limits ozone formation. Other aspects of the environment in which the VOC is emitted, such as nature of the other organics emitted into the airshed (Weir et

al. 1988), the amount of dilution occurring (Carter and Atkinson 1989a), etc., can also be important in affecting VOC reactivities, though investigations of these aspects are more limited.

The fact that incremental reactivities depend on environmental conditions means that no single scale can predict incremental reactivities, or even ratios of incremental reactivities, under all conditions. Thus the concept of a "reactivity scale" oversimplifies the complexities of the effects of VOC emissions on ozone formation. Nevertheless, for some regulatory applications, the only practical alternative to using a reactivity scale is either ignoring reactivity entirely and regulating all VOCs equally – and thus providing no incentives to reduce reactivities of emissions – or using some arbitrary criterion to classify VOCs for regulatory purposes. Which of these alternatives is the least undesirable is a policy issue which is beyond the scope of this paper. However, if the policy is adopted to use a VOC reactivity scale, the scientific issue becomes how one would develop a scale whose use would result in the greatest overall air quality improvement for the range of conditions where it will be applied.

An example of a case where the decision was made to utilize a reactivity scale in a regulatory application is the "Low Emissions Vehicle and Clean Fuels" regulation which was recently adopted in California (CARB, 1990). In 1989, the California Advisory Board on Air Quality and Fuels that Board concluded that increased use of cleaner fuels could be achieved by adopting air-quality based emissions standards (California Advisory Board, 1989; Croes et al, 1992). Around the same time, the staff of the California Air Resources Board (CARB) recommended using reactivity of vehicle exhausts as the basis for comparing air quality impacts of different fuels (CARB, 1989). In 1990, the CARB implemented these recommendations by incorporating reactivity adjustments in the vehicle exhaust emissions standards in the above-referenced regulation. In this regulation, non-methane organic gas exhaust standards for alternative fuels are determined using "reactivity adjustment factors" (RAFs) which are intended relate the differences in ozone formation potential of the exhausts compared to that of conventionally fueled vehicles (CARB 1990). The regulation as presently adopted utilizes the "maximum incremental reactivity" (MIR) scale developed by the author to calculate these RAFs.

In this paper, we describe the development of the MIR scale and the results of investigating alternative approaches for deriving VOC reactivity scales for applications where use of such a scale is required. For this purpose, a set of 39 idealized single day ozone pollution scenarios, each representing a different urban area in the United States, was taken as a representative distribution of ozone pollution episodes, and these were then used as the basis of deriving 18 different reactivity scales, which included the MIR scale as adopted by the CARB.

These different reactivity scales were based on 3 different methods for quantifying ozone impacts and on 6 different approaches for dealingwith the dependencies of reactivity on environmental conditions. The predictions of these scales are compared, and their advantages, disadvantages and relative appropriateness for use in control strategy applications are discussed.

METHODS

This paper uses frequent references to a number of specialized terms and abbreviations. To assist the reader in following this discussion, Table 1 gives a summary of these terms and abbreviations. These are discussed in more detail below.

Scenarios Used for Reactivity Assessment

The development of a comprehensive set of pollution scenarios representing a realistic distribution of ozone pollution conditions requires an analysis of the range of conditions in airsheds where ozone is a problem. This is beyond the scope of this study. However, an extensive set of idealized pollution scenarios has been developed for a number of urban areas for conducting EKMA model analyses of effects of ROG and NO_x controls on ozone formation (e.g., see Gipson et al., 1981; Gipson and Freas, 1983; EPA, 1984; Gery et al., 1987; Bauges, 1990). The EKMA modeling approach involves use of single-cell box models to simulate ozone formation in one day episodes. Although such models cannot represent realistic pollution episodes in great detail, they can represent dynamic injection of pollutants, time-varying changes of inversion heights with entrainment of pollutants from aloft as the inversion height increases throughout the day, and time-varying photolysis rates, temperatures, and humidities (Gipson et al, 1981; Gipson, 1984; EPA, 1984). Thus they can represent a wide range of chemical conditions which may affect predictions of effects of ROG and NO_x control on ozone formation. These chemical conditions are the same as those affecting VOC reactivity. Therefore, at least to the extent they are suitable for their intended purpose, an appropriate set of EKMA scenarios should also be suitable for assessing methods to develop reactivity scales encompassing a wide range of conditions.

Base Case Scenarios.

The set of EKMA scenarios used in this study were based on those developed by the United States EPA for determining, for planning purposes, how various ROG and NO_x control strategies would affect ozone nonattainment in various areas of the country (Bauges, 1990). For this purpose, Bauges (1990, 1991) selected 39 urban areas in the United States based on geographical distribution and coverage of ozone nonattainment areas and based on the availability of the ambient non-methane organic carbon (NMOC) and the local climatological data needed to provide input into the model. For each area, an episode was selected based on its

Table 1. Summary of terms and abbreviations.

Types of Scenarios	
Scenario	A model for an air pollution episode which can be represented in the EKMA model formulation
Base Case Scenario	A scenario designed to represent a specific ozone exceedence episode in an area of the United States.
Maximum Reactivity (MIR) Scenario	A scenario where the NO_x emissions are adjusted to yield highest VOC incremental reactivities
Maximum Ozone (MOR) Scenario	A scenario where the NO_x emissions are adjusted to yield the highest peak ozone concentration.
Equal Benefit (EBIR) Scenario	A scenario where the NO_x emissions are adjusted so VOC and NO_x reductions are equally effective in reducing O_3.
Averaged Conditions Scenario	A scenario whose conditions represent the average of the conditions of the base case scenarios
Scenario Characteristics	
Base ROG	The mixture of reactive organic gases (ROGs) input in the scenario except for biogenic VOCs or VOCs present aloft.
NO_x Availability	The condition of whether NO_x is limiting O_3 formation or whether NO_x is in excess, and the degree to which this is the case. NO_x conditions as they affect reactivity.
NO_x/NO_x^{MOR} ratio	The ratio of NO_x inputs to the NO_x inputs of the maximum ozone scenario. A way to quantify NO_x availability.
IntOH	The effective integrated OH radical levels relating a VOC's kOH to its kinetic reactivity (see Equation IV)
Measures of Reactivity	
kOH	Rate constant for reaction with OH radicals.
Kinetic Reactivity	Fraction of the VOC which reacts in the scenario.
Mechanistic Reactivity (MR)	Amount of ozone formed caused by adding a VOC relative to the amount of VOC which reacted.
Incremental Reactivity (IR)	Amount of ozone formed caused by adding a VOC relative to the amount of VOC added. (Equation I)
Relative Reactivity (RR)	The Incremental reactivity of the VOC relative to the incremental reactivity of the base ROG (Equation II).

Table 1. (continued)

Measures of Reactivity (continued)	
O_3 Yield Reactivity	Reactivity based on the effect of the VOC on the maximum amount of ozone formed.
IntO_3 Reactivity	Reactivity based on the effect of the VOC on the O_3 concentration integrated over time.
IntO_3>90 Reactivity	Reactivity based on the effect of the VOC on the sum of the O_3 concentrations for each hour when $O_3 \geq$ 90 ppb.
Reactivity Scales	
Adjusted NO_x Scales	Scales derived from incremental reactivities in scenarios with a specified condition of NO_x availability.
MIR Scale MOIR Scale EBIR Scales	The adjusted NO_x scales consisting of the average of ozone yield reactivities in the MIR, MOR, or EBIR scenarios.
Base Case Scales	Relative reactivity scales based on incremental reactivities in scenarios where NO_x inputs were not adjusted.
Base(AR) Scales	Base case scales derived using the averaged ratio method. Averages of the relative reactivities in the base case scenarios.
Base(L1) Scales	Base case scales derived using the least squares error method #1. Minimizes the change in ozone caused by substituting the base ROG for the VOC based on the scale.
Base(L2) Scales	Base case scales derived using the least squares error method #2. Minimizes the change in ozone caused by substituting the VOC for the Base ROG based on the scale.
Other	
Null test	A model simulation where one VOC or mixture of VOCs is replaced by another in a proportion which a reactivity scale predicts would have no effect on ozone. The resulting change in ozone is a way of measuring the error of a reactivity scale in a scenario.
LSE RAF	A reactivity adjustment factor (RAF) for an alternative exhaust mixture which minimizes the sum of squares change in ozone in a null test where the emissions of the standard exhaust is replaced by emissions of the alternative exhaust multiplied by a factor of 1/RAF.

representatives of the ozone design value for the city, which is usually the fourth highest ozone day if three complete years of ozone data are available (Bauges, 1990). The initial NMOC and NO_x concentrations in the scenarios were based on the median of all levels measured during all days exceeding 0.124 ppm O_3 or the top ten episodes if more than ten exceedences were measured during the NMOC sampling period. Ozone concentrations aloft were based on downwind measurements made just after the morning increase in the mixing height. The mixing height inputs were prepared based on upper air soundings recommended by the EPA EKMA guidance documents (EPA, 1984). A constant 30 ppb of NMOC aloft was assumed in all scenarios. Hourly emissions by county were obtained from 1985 NAPAP emissions inventory (Gipson, 1991). Biogenic emissions estimates were also included; with separate estimates being made for isoprene, α-pinene and "unknowns". The scenarios also had estimates of initial and emitted CO, and hourly temperature and humidity values. The major characteristics of each of these scenarios are listed in Table 2. Complete tabulations of the scenario conditions and listings of the data files as received from Bauges are given in Appendix B to this report.

Several changes were made to these EPA scenarios based on discussions with the California ARB staff and members of the ARB's reactivity advisory panel (Croes, 1991; CARB, 1991). Based on a suggestion by Pitts (private communication), and analyses of ambient nitrous acid (HONO) measurements (Croes and Carter, 1991), 2% of the initial NO_x and 0.1% if the emitted NO_x in all the scenarios was assumed to be converted to HONO. Methane was assumed to be constant at the global background value of 1.79 ppm. NO_x aloft was assumed to be zero rather than the EPA's default of 2 ppb. The solar light intensities and spectral distributions used to calculate rates of photolysis reactions were those calculated by Jeffries (private communication, 1991) for 640 meters, the approximate mid-point of the mixed layer during daylight hours. The composition of the NMOCs entrained from aloft was derived based on the analysis of aircraft data conducted by Jeffries et al. (1989), and is the same as used by Carter (1991).

Consistent with the treatment in original EPA scenarios (Bauges 1991), the same NMOC composition profile was used to represent the initial and emitted anthropogenic NMOCs for all scenarios. The profile used in this study was developed by Croes (presonal communication, 1991) based on an analysis of ambient hydrocarbon and aldehyde measurements from the EPA data base (Jeffries et al. 1991, and references therein) and obtained from the 1987 Southern California Air Quality Study (SCAQS) (Croes et al., 1993; Lurmann et al. 1992). The hydrocarbons was based on the 1987-88 all-city profile derived from the measurement data of Lonneman (Jeffries et al., 1991), while the oxygenates were based on the SCAQS data (Croes et al. 1993; Lurmann et al. 1992). (The EPA data were preferred for the hydrocarbons because the data set is more robust and very similar to the

Table 2. Summary of conditions of the EPA base case scenarios.

Scenario		Calc. O_3^{max} (ppb)	ROG/NO_x	NO_y/ NO_x^{MOR}	Final H [M]	Input flux (m.mol-m^2) (% emitted)				Aloft O_3 (ppb)
City, State	Date					HC		NOx		
Atlanta, GA	6/6/88	163	7.25	0.79	2146	11.76	(44%)	1.62	(56%)	63
Austin, TX	9/9/88	162	9.30	0.58	2108	11.22	(17%)	1.21	(39%)	85
Baltimore, MD	7/7/88	275	5.15	1.20	1169	16.79	(42%)	3.26	(58%)	84
Baton Rouge, LA	4/26/88	211	6.83	1.02	968	11.13	(44%)	1.63	(73%)	62
Birmingham, AL	7/31/87	223	6.94	0.62	1770	12.83	(9%)	1.85	(33%)	81
Boston, MA	6/16/88	182	6.50	0.66	2598	14.26	(52%)	2.19	(57%)	105
Charlotte, NC	6/8/88	137	7.79	0.36	3046	7.46	(47%)	0.96	(52%)	92
Chicago, IL	8/11/88	251	11.63	0.59	1392	24.97	(33%)	2.15	(59%)	40
Cincinnati, OH	8/18/88	183	6.37	0.83	2816	17.29	(34%)	2.71	(35%)	70
Cleveland, OH	7/5/88	220	6.62	1.07	1650	15.68	(51%)	2.37	(50%)	89
Dallas, TX	9/9/87	167	4.74	1.39	2250	17.51	(49%)	3.70	(72%)	75
Denver, CO	7/26/88	172	6.33	1.25	3358	29.33	(57%)	4.64	(64%)	57
Detroit, MI	8/2/88	217	6.82	0.86	1844	17.29	(49%)	2.54	(55%)	68
El Paso, TX	9/7/88	162	6.59	1.13	2000	12.27	(15%)	1.86	(23%)	65
Hartford, CT	7/8/88	160	8.39	0.53	2318	10.71	(25%)	1.28	(30%)	78
Houston, TX	8/26/88	266	6.08	1.05	1748	25.47	(32%)	4.19	(55%)	65
Indianapolis, IN	7/28/88	187	6.64	1.00	1675	12.06	(41%)	1.82	(68%)	52
Jacksonville, FL	5/7/87	141	7.62	0.72	1485	7.73	(37%)	1.01	(59%)	40
Kansas City, MO	8/7/87	146	7.09	0.67	2200	9.07	(26%)	1.28	(39%)	65
Lake Charles, LA	7/26/88	257	7.42	0.74	457	6.96	(27%)	0.94	(75%)	40
Los Angeles, CA	9/3/88	483	7.59	1.07	503	23.05	(29%)	3.04	(30%)	100
Louisville, KY	6/13/88	191	5.53	0.92	2518	13.74	(40%)	2.48	(78%)	75
Memphis, TN	6/24/87	205	6.78	0.75	1750	14.90	(24%)	2.20	(45%)	58
Miami, FL	4/22/87	125	9.63	0.45	2720	9.47	(25%)	0.98	(38%)	57
Nashville, TN	6/22/86	155	8.05	0.49	1608	7.36	(23%)	0.91	(63%)	50
New York, NY	6/22/88	317	8.09	0.82	1512	39.19	(48%)	4.85	(50%)	103
Philadelphia, PA	7/29/88	212	6.19	1.03	1800	19.01	(75%)	3.07	(76%)	53
Phoenix, AZ	9/9/88	242	7.58	1.05	3250	39.87	(2%)	5.26	(3%)	60
Portland, OR	6/29/87	152	6.46	0.76	1575	6.23	(53%)	0.96	(66%)	66
Richmond, VA	7/10/88	212	6.18	0.90	1932	16.36	(78%)	2.65	(84%)	64
Sacramento, CA	7/23/88	184	6.59	0.93	1103	7.40	(36%)	1.12	(45%)	60
St Louis, MO	7/8/88	269	6.08	1.20	1625	25.63	(81%)	4.21	(86%)	82
Salt Lake City, UT	7/22/88	173	8.47	0.66	2150	10.69	(22%)	1.26	(32%)	85
San Antonio, TX	9/26/88	119	3.92	1.17	2308	6.00	(46%)	1.53	(60%)	60
San Diego, CA	10/3/88	169	7.09	1.06	850	7.67	(33%)	1.08	(37%)	90
San Francisco, CA	5/20/88	167	4.78	1.97	650	25.01	(77%)	5.24	(85%)	70
Tampa, FL	4/23/87	192	4.36	1.25	991	7.90	(29%)	1.81	(67%)	68
Tulsa, OK	7/22/86	201	5.31	1.01	1830	14.86	(29%)	2.80	(42%)	70
Washington, DC	7/30/88	250	5.32	0.92	1421	13.48	(66%)	2.54	(81%)	99
Averaged Conditions		206	6.57	0.91	1823	15.38	(60%)	2.34	(46%)	70

SCAQS hydrocarbon data, while the SCAQS oxygenate data were preferred because they include measurements for the higher oxygenates which are not in the EPA data base, but are consistent with the EPA data in terms of formaldehyde and acetaldehyde levels.) The oxygenates constituted 4.5% of initial and emitted NMOC's, of which slightly under half were formaldehyde and acetaldehyde. The NMOC inputs in the EKMA scenarios were increased by 4.7% to correct for the fact that the oxygenates are not included in the ambient measurements used to derive the NMOC inputs for these EKMA scenarios. A brief summary of the major classes

Table 3. Percentages of major VOC classes in the base ROG mixture, and their contributions to carbon reacted and to the incremental reactivities of the ROG mixture in the MIR, MOIR and EBIR scales.

	Carbon Present	Carbon Reacted	Incremental React'y MIR	MOIR	EBIR
Alkanes	51%	40%	18%	28%	33%
Alkenes	15	20	31	32	35
Aromatics	27	30	42	31	22
Oxygenates	4	5	9	8	9

of compounds in this base ROG mixture is given in the first two columns in Table 3. (The data in the other columns are discussed later.)

No claim is made as to the accuracy of these scenarios in representing any real episode, though clearly they were developed with an attempt to make their input data and predictions as consistent as possible with the available (though generally limited) data. However, even if they are not accurate in representing their particular episodes, they represent the EPA's best efforts to represent, as accurately as possible given the available data and the limitations of the formulation of the EKMA model, the range of conditions occurring in urban areas throughout the United States. For the purpose of investigating reactivity scales, it is more important that the scenarios represent a realistic distribution of chemical conditions than any one accurately representing the details of any particular episode.

These scenarios are referred to as "base case" to distinguish them from the scenarios derived by adjusting NO_x inputs to yield standard conditions of NO_x availability as discussed below.

Adjusted NO_x Scenarios.

It has been shown previously that incremental reactivities – and even ratios of incremental reactivities – can depend significantly on the NO_x levels in the scenarios (E.g., Dodge, 1984; Carter and Atkinson, 1989a; Carter, 1991). This is because NO_x is required for ozone formation, and if NO_x is consumed before the end of the episode or simulation, then VOCs cannot achieve their full ozone formation potential. Table 2 shows that the NO_x inputs and the ROG/NO_x ratios vary widely among the 39 EPA scenarios, suggesting that NO_x availability, and thus incremental reactivities, are also highly variable. However, if the NO_x inputs to these scenarios were adjusted to yield consistent conditions of NO_x availability, one might expect the incremental reactivities, or at least the ratios of incremental reactivities, to be much less variable. If so, the set of incremental reactivities (or reactivity ratios) so obtained may provide a general reactivity scale which is at least applicable to that particular condition of NO_x

availability. Comparing different reactivity scales for different NO_x conditions would provide a systematic means to assess how reactivity scales, and control strategies based on them, would vary with NO_x.

To develop a set of scenarios for this purpose, one needs an appropriate means to quantify NO_x availability, or at least appropriate criteria to establish equivalency in NO_x conditions. NO_x availability is determined both by the amount of NO_x input into the scenario and by the rate of which it is consumed. The ROG/NO_x ratio is obviously an important factor affecting this, but it is not the only one. For example, light intensity, temperature, and the reactivity of the ROGs present will also affect the rate at which NO_x is removed, and thus different scenarios with the same ROG/NO_x ratio may have significantly different conditions of NO_x availability. Because of this, the amount of NO_x input or the ROG/NO_x ratio are not by themselves useful for measuring NO_x availability or establishing equivalency or comparability in NO_x conditions.

A more reliable way to establish comparability in NO_x conditions is to assess similarities or differences in sensitivities, both in sign and magnitude, of ozone formation to changes in NO_x and ROG inputs. If one examines how these sensitivities change as NO_x inputs are varied while holding other scenario conditions constant, we find that a consistent pattern is observed for essentially all scenarios. This is illustrated in Figure 1, which gives plots of the maximum ozone concentration and of the sensitivity of ozone to fractional changes in ROG and NO_x inputs against NO_x input for the conditions of the "averaged conditions" (see below) scenario. Such plots for the other scenarios look essentially the same. In all cases there is a NO_x level where the ROG input has the highest and most positive effect on ozone which is near or the same as the point where the effect of NO_x is the most negative, there is a lower NO_x level which yield the maximum ozone concentration and where the effect of NO_x on ozone changes sign, and there is a yet lower NO_x level where the effects of fractional changes of VOC and NO_x on ozone formation are equal. (These points are designated on the plot using the terminology discussed below.) Although these three points in general occur at different NO_x inputs or ROG/NO_x ratios for conditions of different scenarios, they clearly represent consistent NO_x conditions at least in terms of how ozone formation is affected by ROG and NO_x changes. Thus, these served as the basis for deriving the adjusted NO_x scenarios for this study.

In the "Maximum Incremental Reactivity" (MIR) scenarios, the NO_x inputs are adjusted so that the base ROG mixture had the highest incremental reactivity. This represents NO_x conditions where emissions of VOCs have the greatest effect on ozone formation, and also where NO_x has the strongest ozone inhibiting effect. Note also that MIR conditions can be thought of representing approximately the highest NO_x levels which are relevant in considering control strategies for

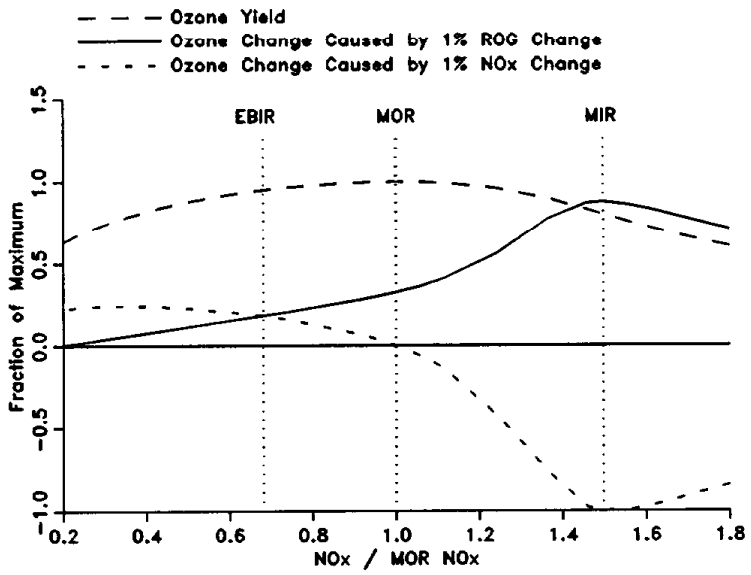

Figure 1. Qualitative dependencies on NO_x inputs of maximum ozone and of relative changes in ozone caused by 1% changes in total ROG or total NO_x emissions for the "Averaged Conditions" Scenarios. NO_x inputs are shown relative to NO_x inputs which give maximum ozone yields.

ozone, because ozone becomes suppressed if NO_x inputs are increased significantly above this level.

In the "Maximum Ozone Reactivity" (MOR) scenarios, the NO_x inputs are adjusted to yield the highest peak ozone concentration. This represents the dividing line between conditions where NO_x is in excess and where ozone is NO_x limited, or the "ridgeline" on ozone isopleth plots (Dodge, 1977). It is also, by definition, the optimum NO_x condition for ozone formation.

In the "Equal Benefit Incremental Reactivity" (EBIR) scenarios, the NO_x inputs are adjusted so that the effect on ozone of a given percentage incremental change in ROG input is the same as the effect of an equal percentage change in NO_x. In other words, this is the point where the incremental reactivity of the base ROG mixture, multiplied by the total amount of ROG input (excluding aloft or biogenic ROGs), equals the incremental reactivity of NO_x, multiplied by the amount of NO_x input. These are refereed to as equal benefit scenarios because a NO_x reductions and VOC reductions are of equal benefit in reducing ozone. It represents the lowest NO_x conditions where VOC control is of equal or greater effectiveness for reducing ozone than NO_x control.

In each of these three cases, the NO_x adjustment was done by varying both the initial NO_x and the emitted NO_x by the same factor. The exact NO_x input level where ozone or base ROG were maximized, or where the equal benefit point occurred, were determined to within 1% by an iterative procedure where the ozone and the derivatives of ozone with respect to ROG or NO_x were calculated and then fit to polynomial curves near the points of interest.

Averaged Conditions Scenarios.

It is useful for sensitivity studies and example calculations to have a single scenario or set of scenario conditions which can be taken as being representative of the larger set. For this purpose, we derived an "averaged conditions" scenario from the averages of all the relevant inputs of the 39 base case scenarios. The inputs which were averaged to derive this scenario included the latitude, longitude, initial and aloft ozone, CO, biogenic levels, aloft hydrocarbon levels, fractions of total non-biogenic and non-aloft ROGs present initially, fractions of total NO_x present initially, hourly emission fluxes of ROG, NO_x, biogenics, and CO, and hourly temperatures, humidities, and inversion heights. The major inputs for this scenario are also given in Table 2. The MIR, MOR, or EBIR versions of this scenario are determined using the exact same procedure as discussed above for the base case scenarios.

A number of calculations were conducted to assess how scenario conditions other than NO_x inputs affect incremental and relative reactivities. These involved starting with the averaged conditions scenario, then modifying some input such as the base ROG composition or the initial HONO. The NO_x inputs were then adjusted to derive the MIR, MOR, or EBIR versions. Comparing results from these with results from the corresponding adjusted NO_x averaged conditions scenarios allows effects of the varied scenario conditions to be assessed on an equal NO_x availability basis. Otherwise, the effect of the variation on NO_x availability may dominate the result.

Calculation of Reactivities in a Scenario.

Incremental Reactivities.

Incremental reactivities in a given scenario (whether base case or adjusted NO_x) are calculated by conducting model simulations of ozone formation in the scenario, and then repeating the calculations with a small amount of the test VOC added. The amount of test VOC added depended on how rapidly it reacted in the scenario, being determined such that the amount reacted was equivalent to daily emissions of 0.01 mmol m^{-2} of reacting VOC. Test calculations showed that this is well within the linear range where incremental reactivities are independent

of the amount of VOC added, yet is sufficient for the effect of the added VOC to be large compared to numerical errors in most cases. The stepwise numerical error tolerance used in the simulations was set such that the uncertainties in the mechanistic reactivities due to numerical errors were less than 0.05 mol of O_3 per mole of VOC reacted. This is small compared to the magnitudes of mechanistic reactivities of most VOCs (Carter and Atkinson, 1989a, see also below). The incremental reactivities are then calculated by determining the change in ozone formed in the two calculations, and dividing it by the amount of test VOC added, as shown in Equation (I), above.

The incremental reactivity of a VOC depends on how the amount of ozone formed in the scenario (the numerator in Equation I) is quantified. Ozone formation can be quantified in a number of ways, including the maximum ozone concentration, the number of moles (or mass) of ozone formed, the ozone level integrated over time, or the extent and/or length of time which ozone exceeds some air quality standard. Three quantifications of ozone are used in this work, each yielding a different incremental reactivity for a VOC in a scenario. In all cases, the amount of VOC added (the denominator) is quantified as the number of moles carbon or mass of VOC introduced into the scenario per unit area.

"Ozone yield" reactivities are based on the maximum number of moles or mass of ozone formed in the scenario, i.e., the moles or grams of O_3 per unit area at the time of the maximum ozone concentration. This gives the same ratios of incremental reactivities as reactivities calculated from peak ozone concentrations, but is preferred because if expressed in molecular units it they have a more fundamental chemical meaning, being molecules of ozone formed per VOC carbon atom emitted. This quantification also permit magnitudes of reactivities in scenarios with differing dilutions to be compared on the same basis. Previous recent studies of incremental reactivity (e.g., Dodge, 1984; Carter and Atkinson, 1987; 1989a; Carter, 1989b; Chang and Rudy, 1990; Lowi and Carter, 1990) have all been based on ozone yield or peak ozone concentration reactivities.

Integrated Ozone ($IntO_3$) reactivities are based on the ozone concentrations integrated over time. They can be different from ozone yield reactivities because if two VOCs give the same maximum ozone concentration when added in equal amounts in the scenarios, but one causes ozone to be formed earlier, their ozone yield incremental reactivities would be the same, but their $IntO_3$ reactivities would be different. $IntO_3$ reactivities have units such as ppm-hours O_3 per gram VOC emitted per unit area, but are always presented in this work in terms of relative reactivities (see below), which are unitless.

An ozone quantification of more direct interest for regulatory applications is the extent to which the ozone exceeds the applicable air quality standard, and the length of time of the exceedence. One way to measure this is the integrated

ozone concentration for the times of the exceedences. In this work, this is approximated by the sum of the hourly ozone concentrations for the times where the ozone exceeds the standard in the calculations without the added VOC. (The times when the standard is exceeded in the calculations with the added VOC would be the same if the amount of VOC added were sufficiently small, as is ideally the case in incremental reactivity calculations.) Since at present the greatest interest in applying reactivity scales is in California, the ozone standard used in this work is the California standard of 0.09 ppm. Incremental reactivities computed from effects of the VOC on integrated O_3 over 90 ppb ($Int O_3$>90 reactivities) have the same units as $Int O_3$ reactivities, but are presented here as unitless relative reactivities.

Relative Reactivities.

For control strategy purposes, the ratios of incremental reactivities for one VOC relative to others is usually of greater relevance than the incremental reactivities themselves. Ratios of reactivities should be less variable among different scenarios than absolute reactivities, particularly for $Int O_3$ and $Int O_3$>90 reactivities, which are not unitless and whose absolute magnitudes depend on the amounts of ozone formed and the amounts of VOCs emitted into the various scenarios.

To define a relative reactivity scale, one needs to select a VOC to use as the standard. For example, Chameides et al. (1992) uses propene, Russell (1990) used carbon monoxide, and Derwent and Jenkins (1991) used ethylene for this purpose. In this work, we will use the base case ROG mixture, i.e., the mixture used in the model simulations to represent the initially present and emitted NMOC's, as the standard. Thus,

$$\text{Relative Reactivity of a VOC} = \frac{\text{Incremental Reactivity of the VOC}}{\text{Incremental Reactivity of Base ROG}} = \text{Change in Base ROG emissions which would have the same effect on ozone formed as a one unit change in emissions of the VOC} = \left[\text{Change in VOC emissions which would have the same effect on ozone formed as one unit change in emissions of the base ROG}\right]^{-1} \quad \text{(II)}$$

Some of the other ways of thinking of relative reactivity, which are relevant to the assessment of methods of determining multi-scenario reactivity scales as discussed below, are also indicated in Equation (II). When defined in this way, the VOC's relative reactivity measures the effect on ozone of changing the emissions of this VOC compared to the effect changing the emissions of all VOCs equally.

Kinetic and Mechanistic Reactivities.

To provide a basis for examining in more detail how differing aspects of VOC reaction mechanisms and scenario conditions affect reactivity, it is useful to consider incremental reactivity as being the product of the "kinetic" and the "mechanistic" reactivities. The kinetic reactivity is the fraction of the emitted VOC which undergoes chemical reaction in the scenario, while the mechanistic reactivity is the change in ozone formed caused by adding the VOC, divided by the amount which reacts, or the incremental reactivity divided by the kinetic reactivity.

$$\begin{aligned} \text{Incremental Reactivity} &= \text{Kinetic Reactivity} \cdot \text{Mechanistic Reactivity} \\ \frac{\text{Ozone Formed}}{\text{VOC Emitted}} &= \frac{\text{VOC Reacted}}{\text{VOC Emitted}} \cdot \frac{\text{Ozone Formed}}{\text{VOC Reacted}} \end{aligned} \qquad \text{(III)}$$

These two components of incremental reactivity each are affected by different aspects both of the VOC reaction mechanism and the scenario conditions, and thus are often more straightforward to estimate, or to assess factors affecting them, than the incremental reactivity.

The kinetic reactivities are functions only of the VOC's relevant rate constants and the levels of the radicals and species in the scenarios which react with the VOCs. Many VOCs react in the atmosphere to a significant extent only with OH radicals, and in those cases the kinetic reactivities depend only on the VOC's OH rate constant (kOH) and on the OH levels in the scenarios. As discussed by Carter and Atkinson (1989a), the kinetic reactivity can then be approximated by

$$\text{Kinetic Reactivity} = \text{Fraction Reacted} \simeq 1 - e^{-kOH \cdot IntOH} \qquad \text{(IV)}$$

$$\simeq kOH \cdot IntOH \quad (\text{if } kOH \ll IntOH^{-1}) \qquad \text{(V)}$$

where IntOH is a scenario-dependent parameter which reflects primarily the overall integrated OH radical levels of the scenario. This simple relationship does not hold for VOCs, such as alkenes, which also react to a non-negligible extent with ozone, or for those, such as aldehydes and ketones, which also photolyze. But the factors involved in considering kinetic reactivities for such compounds are analogous.

Mechanistic reactivities measure the change in ozone resulting when a given amount of the VOC reacts, independently (to a first approximation) to how rapidly it reacts. This provides a means of factoring out the wide variation of reaction rates when assessing mechanistic and environmental effects of VOCs on ozone

formation. Mechanistic reactivities are determined by such factors of the VOC's reaction mechanism as the as number of conversions of NO to NO_2 which occur during its oxidation process, whether the VOC's reactions enhance or inhibit radical or NO_x levels, and the reactivities of the products they form. They are also strongly affected by the conditions of the scenario such as NO_x availability and other factors which affect the overall efficiency of ozone formation (Carter and Atkinson, 1989a). Depending on the conditions of the scenario and the nature of the reaction mechanisms, mechanistic reactivities can range from negative values (indicating the VOC's reactions actually reduce overall ozone formation) to values as high as over 10 moles of ozone formed per mole of carbon reacted (Carter and Atkinson, 1989a).

The kinetic reactivity of a VOC in a scenario is calculated by determining the final concentration of the VOC in the scenario which would occur if it did not react, then subtracting from this the final concentration when it does react, and dividing this by the final concentration of the VOC if it did not react. In this work, the kinetic reactivities of the various VOCs were calculated in this manner, except as follows: For VOCs which react only with OH radicals, the kinetic reactivity is determined from the VOC's kOH from the dependence of the kinetic reactivities on kOH which is determined separately for each scenario. For alkenes other than ethene, the kinetic reactivities were estimated as if they reacted only with OH radicals, which is an approximation but not a significant one because the higher alkenes react so rapidly that their kinetic reactivities are near unity in any case. (Note that approximating kinetic reactivities in alkenes only affects their calculated mechanistic reactivities, not their incremental or relative reactivities.) The kinetic reactivities for the other compounds which are represented explicitly in the model (e.g., ethene, formaldehyde, acetone, etc.) were calculated explicitly.

The mechanistic reactivities for most VOCs were calculated from the ratios of the incremental to the calculated kinetic reactivities. For some VOCs which react only with OH radicals in the mechanism, the mechanistic reactivities were derived from mechanistic reactivities of "pure mechanism" species (Carter and Atkinson, 1989a) using mathematically derived relationships discussed by Carter (1991) and Carter and Atkinson (1989a), and then the incremental reactivities were derived by multiplying the mechanistic reactivity times the kinetic reactivity derived from the VOC's kOH. This latter approach, which is applicable only to VOCs which react only with OH radicals, is mathematically equivalent to calculating the VOC's reactivity components directly (Carter, 1991) in the incremental reactivity limit, but is more sensitive to numerical errors than the direct method. This method was found to give reactivities which agree reasonably well with those calculated directly, but tends to be biased towards overestimating the reactivities, typically by ~5%. Footnotes in the listing of the results for individual VOCs indicate the method used.

Mass-Basis or Carbon-Basis Quantification.

Incremental reactivities can be given either on a per-gram or a per carbon basis, depending on how the VOCs are quantified. For example, ozone yield reactivities could be expressed as either moles ozone per mole carbon emitted, or as grams ozone per gram VOC. It is important to be clear on which quantification is used because this can affect relative reactivities of VOCs, such as formaldehyde or methanol, which have different molecular weights per carbon than the base ROG mixture. In this work, except as noted we will quantify incremental and relative reactivities on a gram basis because that is of more relevant to application to control strategies. However, mechanistic reactivities will be quantified on a moles ozone per carbon basis because this is more directly related to the mechanistic processes. The conversion relationships used are: Ozone yield incremental reactivity: (gm O_3/gm VOC) = (mol O_3/mol C VOC)·48.0·(carbons in VOC)/(molecular weight of VOC); Relative reactivities: (mass basis) = (carbon basis)·14.44·(carbons in VOC)/(molecular weight of VOC). These are based on a molecular weight per carbon of 14.44 for the base ROG mixture and a molecular weight of 48 for ozone..

Derivation of General and Multi-Scenario Reactivity Scales.

The focus of this work is to examine methods for developing generalized reactivity scales reflecting a variety of conditions. Two types of approaches are employed: (1) developing scales reflecting specified conditions of NO_x availability, specifically maximum reactivity (MIR), maximum ozone (MOR), or equal benefit (EBIR) conditions as discussed above, and (2) developing multi-scenario scales using various methods to combine or average reactivities for the set of base case scenarios which is assumed, for the purpose of this study, to represent a realistic distribution of conditions. In each case, separate scales were derived based on the effect on O_3 yield, integrated O_3, or integrated O_3 over 90 ppb. These methods are discussed below.

Adjusted NO_x Scales.

A total of 9 adjusted NO_x scales were derived based on the three conditions of NO_x availability and the three methods for quantifying ozone. In the case of the three ozone yield scales, which are designated the "maximum incremental reactivity: (MIR), "maximum ozone incremental reactivity" (MOIR) and the "equal benefit incremental reactivity" (EBIR) scales, values of kinetic, mechanistic, incremental, and relative reactivity values were derived. In the case of the three $Int O_3$ and the three $Int O_3$>90 scales, only relative reactivities were derived. In all cases, the relative reactivities were derived by averaging the appropriate type of relative reactivity in the corresponding type of adjusted NO_x

scenarios. In the case of the MIR, MOIR, or EBIR scales, the averages of kinetic and the mechanistic reactivities for the various types of adjusted NO_x scenario were determined, and these were combined to yield the incremental reactivities in the scale. Although this latter approach is not equivalent to averaging incremental reactivities, it has the advantage of yielding values of kinetic and mechanistic reactivities to associate with the scales. This is useful for the analysis of mechanistic and environmental effects on reactivity scales as discussed below. In practice, essentially the same results are obtained.

Base Case Scales.

The incremental reactivities would be expected to vary widely among the unadjusted (base case) scenarios because of their wide variation of conditions of NO_x availability. For this reason, only relative base case reactivity scales were derived. However, in most cases relative reactivities were also quite variable among the base case scenarios, and different scales can be obtained depending on the methods used to derive the scales. Three different methods were employed, as discussed below. Combined with the three methods for quantifying ozone, this yielded 9 different base case reactivity scales.

The "average ratio" (AR) method consists of simply averaging the relative reactivities in the base case scenarios, with each scenario being weighed equally. This is the method used to derive the relative reactivities in the adjusted NO_x scales. However, its utility for the base case scales is more problematical because in many cases (particularly for ozone yield reactivities) the quantities being averaged are much more variable. In addition, the fact that this method weighs the relative reactivities in all scenarios equally, despite that fact that ozone is much more sensitive to VOC changes in some scenarios than in others, suggests that this may not give an optimum scale for control applications. A more optimum scale should give greater weight to scenarios which are more sensitive to the quantities being regulated.

The "least squares error" methods are based on minimizing the calculated sum-of-squares change in ozone which would result if a substitution which the scale predicts would have zero effect on ozone were applied throughout the set of scenarios. Model calculations of substitutions which a reactivity scale predicts has no effect on ozone are referred to as "null tests" of the scale. For example, if the relative reactivity of a compound in a scale were 0.5, then the scale predicts that substitution of 2 units of the compound for one unit of the base ROG would result in no net change in ozone. A null test calculation would be a simulation of the effect of this substitution. Since in general relative reactivities varies from scenario to scenario, a null test substitution would cause a change in ozone in at least some of the scenarios no matter what relative reactivity were used. This change can then be thought of as a measure

of the "error" of the reactivity scale for the scenario. The least squares error relative reactivity is the value which minimizes the sum of squares of this error, or change in ozone, resulting from this null test. Note that this method will give greater weight to scenarios where ozone is more sensitive to VOCs because the effects on ozone of using an inappropriate relative reactivity in the substitution would be larger.

Since relative reactivity is defined in terms of the reactivities of the VOC compared to the base ROG, the relevant substitution strategies for deriving these scales would involve either (1) reducing emissions of the VOC and offsetting it by an increase in the emissions of all ROGs, or (2) reducing all ROGs and offsetting it by an increase in the VOC. The two substitutions do not necessarily yield the same relative reactivity scale, as discussed below.

"Least squares error method #1" (L1) is based on minimizing the errors in null tests of ROG for VOC substitutions. If RR^{VOC} is the relative reactivity of a VOC in the scale, then the scale predicts replacing one unit of the VOC emissions with RR^{VOC} units of emissions of the base ROG mixture would result in no change in ozone. If IR_i^{VOC} and IR_i^{ROG} are the incremental reactivities of a given VOC and the base ROG, respectively, in the i'th scenario in a set of scenarios, then the change in ozone in scenario i caused by this substitution, or the error in the scale for scenario i, is $(IR_i^{VOC}-RR^{VOC}\cdot IR_i^{ROG})$. The total sum of squares error for all the scenarios is then given by $\sum_i (IR_i^{VOC}-RR^{VOC}RR_i^{ROG})^2$. The value of RR^{VOC} which minimizes this sum of squares error (obtained setting the derivative of the above to zero and solving for RR^{VOC}) is

$$RR_{L1}^{VOC} = \frac{\sum_i IR_i^{VOC}\cdot IR_i^{ROG}}{\sum_i \left(IR_i^{ROG}\right)^2} = \frac{\sum_i \left(IR_i^{ROG}\right)^2 \cdot RR_i^{VOC}}{\sum_i \left(IR_i^{ROG}\right)^2} \qquad \text{(VI)}$$

Note that solving Equation (IV) is exactly the same problem as finding the slope of the least squares line, forced through zero, which fits plots of $IR_i(VOC)$ against $IR_i(ROG)$.

Note also that Equation (VI) is the same as the weighed average of the relative reactivities in the scenarios, RR_i^{VOC}, computed using $(IR_i^{ROG})^2$ as the weighing factor. Thus scenarios with higher incremental reactivities, i.e., where ozone is more sensitive to VOCs, contribute more to the Base(L1) reactivities than scenarios where ozone is less sensitive to VOCs. This weighing factor is what differentiates this derivation method from the average ratio method.

"Least squares error method #2" (L2) is based on minimizing errors in null tests of VOC for ROG substitutions. In this case, if RR^{VOC} is the relative reactivity of the VOC, then the scale predicts replacing one unit of the total ROG emissions by $1/RR^{VOC}$ units of the VOC would result in no change in ozone. In a manner analogous to the derivation above, this yields

$$RR_{L2}^{VOC} = \frac{\sum_i \left(IR_i^{VOC} \right)^2}{\sum_i IR_i^{VOC} \cdot IR_i^{ROG}} \qquad \text{(VII)}$$

This is the same as finding the slope of the least squares line, forced through zero, fitting plots of IR_i^{ROG} against IR_i^{VOC}.

In most cases, the two derivations of RR^{VOC} yield essentially the same result. Method #2 may seem preferable from a control strategy perspective because most substitutions of interest involve replacing current emissions with some less reactive VOC (e.g., alternative fuel use), rather than using reductions of highly reactive VOCs as credits to allow less restrictions on emissions of all other VOCs. However, note that if RR^{VOC} is derived using method 1 (Equation VI), then the relative reactivities of mixtures would be given by the sum of the relative reactivities of the components times their relative amounts (as is the case for incremental and relative reactivities of mixtures in single scenarios), while this linear summation method for relative reactivities of mixture is not valid for method 2 (Equation VII). In addition, Equation (VII) fails for unreactive VOCs (where $IR_i^{VOC} \equiv 0$), and is highly sensitive to outliers in the distribution for VOCs whose reactivities are distributed evenly around zero. Therefore, method #1 is preferred because it is more tractable mathematically, yields reasonable results for VOCs with reactivities near zero, and is essentially equivalent to method #2 for the positively reactive VOCs which are the most important in affecting ozone formation.

Chemical Mechanism.

The chemical mechanism used in this study is that of Carter (1990), with updates for several VOCs as indicated in footnotes to the reactivity results tabulations, below. A complete listing of the mechanism is given in Appendix A of this report. This mechanism contains rate constant and product yield assignments for over 140 separate "detailed model species", making it the most detailed of all current mechanisms in terms of the number of organic species which can be separately represented. It was evaluated by conducting model simulations of over 500 environmental chamber experiments (Carter and Lurmann 1991). It was found to be able to simulate maximum ozone concentrations and

rates of NO oxidation and ozone formation to within ±30% for 63% of the experiments, and to within ±50% for 85% of the runs, but had a slight bias (~15%) towards overpredicting maximum ozone concentrations in the experiments designed to represent ambient mixtures. This is comparable or slightly better than the performance of the RADM-II (Stockwell et al. 1990) Carbon Bond IV (Gery et al., 1988) mechanisms in simulating the same data base using the same chamber effects model (Carter and Lurmann, 1990; Carter, unpublished results). This is good as can be reasonably expected given our current state of knowledge of atmospheric chemistry and characterization of chamber artifacts (Carter and Lurmann, 1991).

This mechanism is considered appropriate for reactivity calculations because it is at least as up to date as the other available comprehensive mechanisms (Hough, 1988; Gery et al. 1988; Stockwell et al. 1990) and it is the only one designed to represent large numbers of VOCs which has been extensively tested against chamber data. However, its limitations and uncertainties must be recognized. Most of the mechanism represents the state of knowledge as of 1989-1990 and is out of date in some respects. (The effects of implementing some updates are discussed later.) At the time it was developed, the available chamber data were sufficient to test the representation of only ~20 representative VOCs, and the mechanisms for most of the others were derived by extrapolation or estimations (Carter, 1990). In addition, the available chamber data did not provide a good test for the mechanisms for some of these VOCs because the relevant data were sparse, inconsistent, or dominated by chamber artifacts (Carter and Lurmann, 1990, 1991). Although the initial rates of reaction for the individual VOCs are in most cases based on measurements or estimates for the individual compounds, in many cases the other aspects of the mechanisms, such as the amounts of NO to NO_2 conversions and the types of radicals and products formed, are assumed to be the same for large numbers of VOCs which are judged to be chemically similar. Nevertheless, the mechanism incorporates our best present estimates for the reaction mechanisms of the wide variety of VOCs which are emitted into the atmosphere.

The uncertainties in the reaction mechanism obviously must be taken into account when the results of model calculations of reactivities are used to assess ozone control strategies. To aid in such assessments, the master listing of reactivity results given below include footnotes indicating levels of uncertainty in the mechanisms for the various VOCs, and indicates whether new data, which became available after the mechanism was developed, indicate possible biases in the calculated reactivities.

RESULTS AND DISCUSSION

NO_x Availability, Ozone Yields and Base ROG Incremental Reactivity.

Figure 2 shows the distribution plots of the maximum ozone concentrations, two measures of the NO_x levels, and the base ROG incremental reactivities for the various scenarios. The figure shows that there are wide distributions ROG/NO_x ratios for the adjusted NO_x scenarios, indicating that the ROG/NO_x ratios are, by themselves, poor predictors of NO_x availability. A much better predictor is the ratio of the NO_x input to the NO_x input of the MOR scenario, or NO_x/NO_x^{MOR}. This ratio, which is 1 by definition for the MOR scenarios, was found to be narrowly distributed around 1.5 (averaging 1.50±0.05) for the MIR scenarios, and 0.7 (averaging 0.70±0.05) for the EBIR scenarios. On the other hand, it varies widely among the base scenarios, providing a more reliable indication than the variation of the ROG/NO_x ratio that there is indeed a wide variability in NO_x availability among these scenarios. By this measure, most of the base scenarios are between MOR ozone and EBIR conditions. (The average NO_x/NO_x^{MOR} for the base scenarios is 0.9±0.3.) Only a few of these scenarios have NO_x/NO_x^{MOR} ratios close to the MIR range, and only one with NO_x levels higher than this. On the other hand, several scenarios have lower NO_x/NO_x^{MOR} ratios than the EBIR level. Note that the scenarios used in our previous study (Carter, 1991) have a much wider range of NO_x/NO_x^{MOR} ratios than these EPA scenarios.

The maximum ozone levels are very similar under MOR and EBIR conditions, (the latter being only 4% lower than the former), which is expected given the relative insensitivity of ozone to NO_x changes in this range, as shown on Figure 1. The similarity of the distribution of maximum ozone levels in the base scenarios to the distributions for the MOR and EBIR scenarios reflects the fact that most of the base case scenarios are in the MOR to EBIR range. The ozone yields in the MIR scenarios are somewhat lower, though they are all above the California standard of 0.09 ppm, and are above the Federal ozone standard of 0.12 ppm in all but three cases. Thus, while MIR conditions are not optimum for ozone formation, excessive levels of ozone can still be formed.

By definition, the base ROG incremental reactivities are the highest in the MIR scenarios. This decreases rapidly as the NO_x is reduced, with the average decreasing by a factor of 2.7 in going from MIR to MOR conditions, and by another ~40% in going from MOR to EBIR conditions. The distribution of base ROG reactivities in the base scenarios are as expected given the their distribution of NO_x conditions.

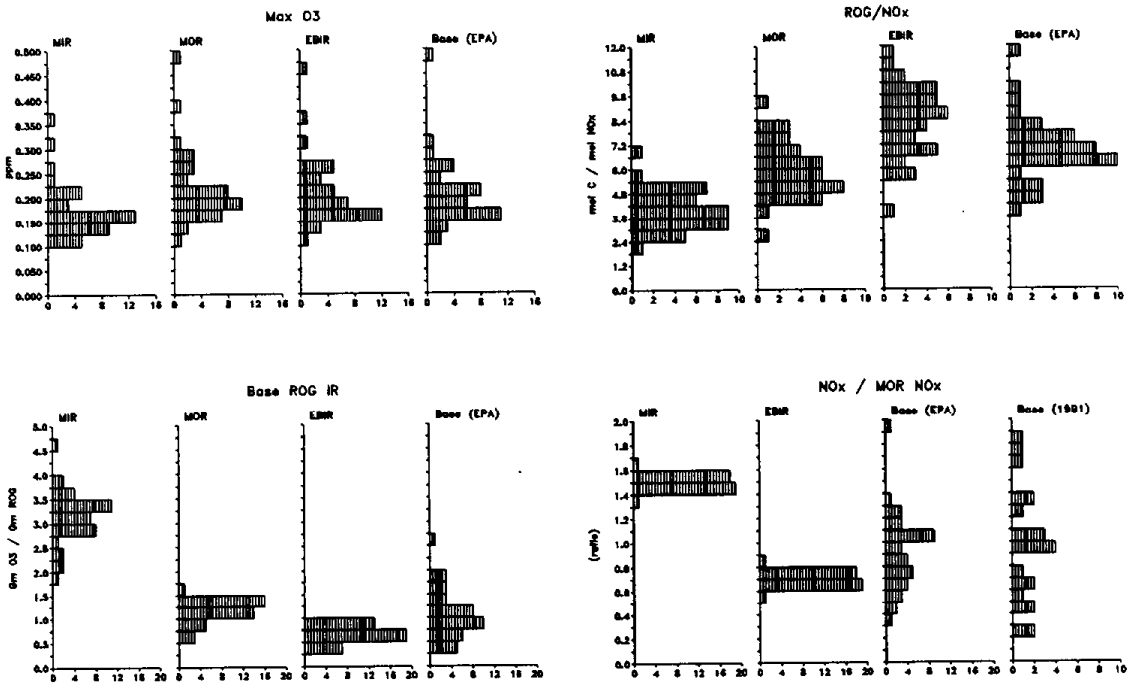

Figure 2. Distribution plots of maximum ozone, the base ROG incremental reactivity, the ROG/NO_x ratio, and the ratio of NO_x inputs MOR NO_x inputs for the MIR, MOR, EBIR and base case scenarios. Base scenarios used by Carter (1991) are shown on the NO_x/NO_x^{MO} plot.

Ozone Yield Reactivity Scales for Fixed NO_x Conditions

Table 4 gives the kinetic, mechanistic, and incremental ozone yield reactivities calculated for the maximum incremental reactivity (MIR), maximum ozone incremental reactivity (MOIR) and the equal benefit incremental reactivity (EBIR) scales. Footnotes to the table give the level of uncertainty in the mechanisms of the various VOCs, and (where applicable) available data concerning their mechanisms which have not yet been incorporated into the mechanisms. The incremental reactivities of the base ROG mixture, which is used as the standard for defining relative reactivities, are also given. These data are discussed below, first in terms of the variability and differences of incremental reactivities and its components, and then in terms the differences and variabilities of the relative reactivities.

Distribution plots of the kinetic, mechanistic, incremental, and relative reactivities of CO among the adjusted NO_x scenarios are given in Figure 3, and distributions of mechanistic and relative reactivities for toluene and

formaldehyde are given on Figures 4 and 5. These show the variability of these components and measures of reactivity among the various adjusted NO_x scenarios, and thus they show the extent to which they are affected by the variability of the non-NO_x-related scenario conditions. Distributions for the base case scenarios are also shown on these figures for comparison.

NO_x Effects and Variations in Kinetic Reactivities.

Kinetic reactivities for slowly reacting compounds which react only with OH, such as CO, tend to be proportional to the compound's OH rate constant and the integrated OH radical levels (IntOH) in the scenarios. Thus, the distributions of the kinetic reactivities of CO shown on Figure 3 are characteristic of the kinetic reactivity distributions for all slowly reacting compounds, and reflect the distributions of IntOH for the scenarios. More rapidly reacting compounds would also have similar distributions except that they are narrower and closer to unity.

Figure 3 and Table 4 shows that the kinetic reactivities of CO and the other slowly reacting compounds are considerably lower, by ~35% on the average, under MIR conditions compared to MOR and EBIR conditions. The lower kinetic reactivities in MIR scenarios is presumably due to their higher NO_x levels, since NO_x is involved in a number of termination reactions. On the other hand, the kinetic reactivities apparently do not increase further to a significant extent as NO_x is reduced from MOR to EBIR levels, presumably because the reduced termination caused by lower NO_x is offset by the increased termination due to HO_2 + HO_2 and other peroxy + peroxy reactions which become more important once NO_x is consumed. However, the wide distributions of kinetic reactivities in the adjusted NO_x scenarios indicate that kinetic reactivities are significantly affected by other factors besides NO_x. Factors such as light intensity, temperature and dilution would also be expected to affect radical initiation and termination rates and thus be of equal or greater significance as NO_x in affecting kinetic reactivities.

NO_x Effects and Variations in Mechanistic Reactivity.

Table 4 and Figures 3-5 show that mechanistic reactivity is the dominant factor affecting how incremental reactivities vary with NO_x. The decline in mechanistic reactivity as NO_x is decreased from MIR to MOR levels is more then enough to offset any increase in kinetic reactivities. In contrast to the case with kinetic reactivities, there is also almost no overlap in the distributions of mechanistic reactivities in the MIR and MOR scenarios; the data on Figures 3-5 are typical in this regard. Thus, at least when NO_x is above MOR levels, NO_x availability dominates over other scenario conditions in affecting mechanistic reactivity. While NO_x is still important in affecting mechanistic reactivities

Table 4 Hydroxyl radical rate constants and kinetic, mechanistic, and incremental reactivities in the adjusted NO_x reactivity scales for various VOCs, with notes concerning the status of the VOC's mechanisms.

Description	kOH [a]	Kinetic Reactivity			Mech. React'y [b]			Incr'l. React'y [c]			Unc. [d]	Doc. [e]
		MIR	MOIR	EBIR	MIR	MOIR	EBIR	MIR	MOIR	EBIR		
Carbon Monoxide	3.52+2	0.035	0.055	0.056	0.91	0.40	0.31	0.054	0.038	0.029	1	1
Alkanes [f]												
Methane	1.28+1	0.0013	0.002	0.002	3.8	1.49	1.10	0.015	0.009	0.007	2	1
Ethane	4.02+2	0.040	0.063	0.064	1.9	0.82	0.60	0.25	0.17	0.122	2	1
Propane	1.71+3	0.16	0.24	0.24	0.93	0.40	0.28	0.48	0.31	0.22	2	1
n-Butane	3.76+3	0.31	0.44	0.45	0.99	0.45	0.32	1.02	0.66	0.47	1	2
n-Pentane	6.03+3	0.45	0.60	0.60	0.70	0.34	0.24	1.04	0.68	0.48	5	2
n-Hexane	8.27+3	0.55	0.71	0.71	0.53	0.27	0.19	0.98	0.65	0.44	5	2
n-Heptane	1.06+4	0.64	0.78	0.78	0.38	0.20	0.128	0.81	0.53	0.33	5	2
n-Octane	1.29+4	0.70	0.83	0.83	0.26	0.146	0.082	0.60	0.41	0.23	5	2
n-Nonane	1.50+4	0.75	0.86	0.86	0.21	0.123	0.066	0.54	0.36	0.19	5	2
n-Decane	1.71+4	0.78	0.88	0.88	0.17	0.104	0.053	0.46	0.31	0.16	7	2
n-Undecane	1.95+4	0.82	0.90	0.90	0.15	0.092	0.045	0.42	0.28	0.136	8	2
n-Dodecane	2.09+4	0.84	0.91	0.91	0.133	0.082	0.039	0.38	0.25	0.120	8	2
n-Tridecane	2.36+4	0.86	0.92	0.92	0.119	0.075	0.035	0.35	0.23	0.110	8	3
n-Tetradecane	2.45+4	0.87	0.93	0.92	0.108	0.069	0.032	0.32	0.22	0.100	8	3
Isobutane	3.46+3	0.29	0.42	0.42	1.25	0.53	0.38	1.21	0.73	0.53	7	2
Neopentane	1.27+3	0.120	0.18	0.19	0.93	0.36	0.23	0.37	0.22	0.144	7	2
Iso-Pentane	5.79+3	0.43	0.59	0.59	0.96	0.44	0.32	1.38	0.87	0.63	7	2
22-Dimethyl Butane	3.46+3	0.29	0.42	0.42	0.84	0.36	0.25	0.82	0.51	0.34	7	2
23-Dimethyl Butane	8.08+3	0.54	0.70	0.70	0.59	0.29	0.21	1.07	0.67	0.48	5	3
2-Methyl Pentane	8.31+3	0.55	0.71	0.71	0.83	0.38	0.26	1.5	0.90	0.61	7	2
3-Methylpentane	8.46+3	0.56	0.71	0.71	0.81	0.40	0.28	1.5	0.94	0.67	7	2
223-Trimet. Butane	6.22+3	0.46	0.61	0.61	0.86	0.38	0.27	1.32	0.79	0.56	7	2
23-Dimethyl Pentane	1.07+4	0.64	0.78	0.78	0.71	0.34	0.24	1.5	0.90	0.63	7	3
24-Dimethyl Pentane	1.02+4	0.62	0.77	0.77	0.86	0.38	0.26	1.8	0.99	0.67	7	3
33-Dimethyl Pentane	4.63+3	0.37	0.51	0.51	0.58	0.27	0.17	0.71	0.46	0.30	7	3
2-Methyl Hexane	1.01+4	0.62	0.77	0.77	0.52	0.26	0.18	1.08	0.68	0.46	7	3
3-Methyl Hexane	1.06+4	0.64	0.78	0.78	0.65	0.32	0.21	1.40	0.83	0.55	7	3
224-Trime. Pentane	5.46+3	0.42	0.57	0.57	0.67	0.28	0.17	0.93	0.54	0.33	7	2
234-Trime. Pentane	1.28+4	0.70	0.83	0.82	0.68	0.33	0.23	1.6	0.92	0.64	7	3
23-Dimethyl Hexane	1.28+4	0.70	0.83	0.82	0.56	0.28	0.19	1.31	0.78	0.53	7	3
24-Dimethyl Hexane	1.28+4	0.70	0.83	0.82	0.64	0.31	0.21	1.5	0.86	0.58	7	3
25-Dimethyl Hexane	1.22+4	0.68	0.82	0.81	0.71	0.34	0.23	1.6	0.93	0.64	7	3
2-Methyl Heptane	1.22+4	0.68	0.81	0.81	0.42	0.22	0.139	0.96	0.59	0.38	7	3
3-Methyl Heptane	1.27+4	0.69	0.82	0.82	0.42	0.22	0.147	0.99	0.62	0.41	7	3
4-Methyl Heptane	1.27+4	0.69	0.82	0.82	0.51	0.25	0.16	1.20	0.70	0.45	7	3
24-Dimethyl Heptane	1.48+4	0.74	0.86	0.85	0.53	0.26	0.17	1.33	0.75	0.49	7	3
225-Trime. Hexane	9.04+3	0.58	0.73	0.73	0.50	0.23	0.148	0.97	0.58	0.37	7	3
4-Ethyl Heptane	1.56+4	0.76	0.87	0.86	0.44	0.22	0.139	1.13	0.64	0.40	7	3
34-Propyl Heptane	1.77+4	0.79	0.89	0.88	0.38	0.19	0.115	1.01	0.56	0.34	8	3
35-Diethyl Heptane	2.12+4	0.84	0.91	0.91	0.41	0.22	0.148	1.17	0.68	0.45	7	3
26-Diethyl Octane	2.33+4	0.86	0.92	0.92	0.42	0.22	0.148	1.23	0.69	0.46	8	3
Cyclopentane	7.62+3	0.52	0.68	0.68	1.33	0.61	0.42	2.4	1.41	0.99	7	2
Methylcyclopentane	1.19+4	0.67	0.81	0.81	1.22	0.56	0.39	2.8	1.6	1.07	7	3
Cyclohexane	1.11+4	0.65	0.79	0.79	0.57	0.27	0.17	1.28	0.74	0.47	7	2
13-Dime. Cyclo. C5	1.27+4	0.70	0.82	0.82	1.07	0.49	0.34	2.5	1.38	0.96	8	3
Methylcyclohexane	1.51+4	0.75	0.86	0.86	0.72	0.34	0.22	1.8	1.00	0.65	5	3
Ethyl Cyclopentane	1.32+4	0.71	0.83	0.83	0.95	0.46	0.31	2.3	1.30	0.89	8	3
Ethylcyclohexane	1.81+4	0.80	0.89	0.89	0.71	0.33	0.22	1.9	1.02	0.66	8	3
1-Et.-4-Me. Cyc. C6	2.07+4	0.83	0.91	0.90	0.81	0.38	0.25	2.3	1.18	0.78	8	3
13-Diet.-Cyc. C6	2.36+4	0.86	0.92	0.92	0.60	0.29	0.20	1.8	0.93	0.62	8	3
13-Diet.-5-Me.Cy.C6	2.63+4	0.89	0.94	0.93	0.63	0.31	0.21	1.9	1.00	0.68	8	3
135-Triet. Cyc. C6	2.92+4	0.90	0.95	0.94	0.54	0.27	0.18	1.7	0.87	0.59	8	3

Table 4 (continued)

Description	kOH [a]	Kinetic Reactivity MIR	MOIR	EBIR	Mech. React'y [b] MIR	MOIR	EBIR	Incr'l. React'y [c] MIR	MOIR	EBIR	Unc. [d]	Doc. [e]
Alkenes												
Ethene	1.24+4	0.69	0.82	0.82	3.2	1.14	0.75	7.4	3.2	2.1	1	4
Propene	3.82+4	0.94	0.97	0.97	2.9	1.14	0.75	9.4	3.8	2.5	4	4
1-Butene	4.56+4	0.96	0.98	0.98	2.7	1.05	0.68	8.9	3.5	2.3	4	4
1-Pentene	4.56+4	0.96	0.98	0.98	1.9	0.74	0.46	6.2	2.5	1.6	7	5
3-Methyl-1-Butene	4.61+4	0.96	0.98	0.98	1.9	0.74	0.46	6.2	2.5	1.6	7	5
1-Hexene	5.37+4	0.97	0.98	0.98	1.33	0.52	0.32	4.4	1.7	1.06	4	5
1-Heptene	5.37+4	0.97	0.98	0.98	1.05	0.41	0.24	3.5	1.38	0.82	8	5
1-Octene	5.37+4	0.97	0.98	0.98	0.81	0.32	0.18	2.7	1.07	0.62	8	5
1-Nonene	5.37+4	0.97	0.98	0.98	0.67	0.26	0.15	2.2	0.89	0.50	8	5
Isobutene	7.46+4	0.98	0.99	0.99	1.6	0.57	0.36	5.3	1.9	1.22	5	4
2-Methyl-1-Butene	8.80+4	0.98	0.99	0.98	1.46	0.56	0.36	4.9	1.9	1.23	7	5
trans-2-Butene	9.24+4	0.98	0.98	0.98	3.0	1.12	0.72	10.0	3.8	2.4	5	4
cis-2-Butene	8.19+4	0.98	0.98	0.98	3.0	1.12	0.72	10.0	3.8	2.4	5	4
2-Pentenes	9.62+4	0.98	0.98	0.98	2.6	0.98	0.62	8.8	3.3	2.1	7	5
2-Methyl-2-Butene	1.26+5	0.99	0.99	0.99	1.9	0.68	0.42	6.4	2.3	1.42	7	5
2-Hexenes	9.62+4	0.98	0.98	0.98	2.0	0.75	0.47	6.7	2.5	1.6	8	6
2-Heptenes	9.62+4	0.98	0.98	0.98	1.7	0.62	0.38	5.5	2.1	1.29	8	6
3-Octenes	9.62+4	0.98	0.98	0.98	1.6	0.59	0.37	5.3	2.0	1.23	8	7
3-Nonenes	9.62+4	0.98	0.98	0.98	1.37	0.51	0.32	4.6	1.7	1.06	8	7
13-Butadiene	9.67+4	0.98	0.98	0.98	3.1	1.20	0.78	10.9	4.2	2.7	8	4
Isoprene	1.46+5	0.99	0.99	0.99	2.6	0.98	0.63	9.1	3.4	2.2	6	4
Cyclopentene	9.74+4	0.98	0.98	0.98	2.2	0.81	0.50	7.7	2.8	1.7	8	8
Cyclohexene	9.82+4	0.98	0.98	0.98	1.7	0.64	0.41	5.7	2.2	1.42	8	8
a-Pinene	7.80+4	0.98	0.99	0.99	0.95	0.37	0.24	3.3	1.28	0.83	5	8
b-Pinene	1.15+5	0.98	0.99	0.98	1.27	0.48	0.31	4.4	1.7	1.08	8	8
Acetylenes												
Acetylene	1.15+3	0.109	0.17	0.17	1.25	0.53	0.40	0.50	0.33	0.25	5	1
Methyl Acetylene	8.90+3	0.58	0.73	0.73	2.0	0.83	0.57	4.1	2.2	1.48	9	9
Aromatics												
Benzene	1.89+3	0.17	0.26	0.26	0.67	0.144	0.046	0.42	0.138	0.04	4	1
Toluene	8.67+3	0.57	0.72	0.72	1.32	0.24	0.013	2.7	0.63	0.03	4	1
Ethyl Benzene	1.04+4	0.63	0.78	0.78	1.18	0.22	0.018	2.7	0.63	0.05	7	1
n-Propyl Benzene	8.81+3	0.57	0.73	0.73	1.03	0.19	0.010	2.1	0.49	0.03	7	1
Isopropyl Benzene	9.54+3	0.60	0.75	0.75	1.04	0.19	0.013	2.2	0.52	0.03	7	1
s-Butyl Benzene	8.81+3	0.57	0.73	0.73	0.93	0.17	0.009	1.9	0.44	0.03	7	1
o-Xylene	2.01+4	0.83	0.91	0.91	2.2	0.59	0.27	6.5	2.0	0.88	4	1
p-Xylene	2.10+4	0.84	0.92	0.92	2.2	0.60	0.27	6.6	2.0	0.90	7	1
m-Xylene	3.46+4	0.93	0.96	0.96	2.4	0.71	0.34	8.2	2.5	1.17	4	1
135-Trime. Benzene	8.44+4	0.98	0.99	0.99	2.9	0.86	0.44	10.1	3.1	1.6	4	1
123-Trime. Benzene	4.80+4	0.96	0.98	0.98	2.6	0.76	0.38	8.9	2.7	1.33	7	1
124-Trime. Benzene	4.77+4	0.96	0.98	0.98	2.6	0.76	0.38	8.8	2.7	1.33	7	1
Tetralin	5.03+4	0.97	0.98	0.98	0.27	0.036	-0.036	0.94	0.129	-0.127	5	1
Naphthalene	3.17+4	0.92	0.95	0.95	0.34	0.026	-0.068	1.17	0.09	-0.24	5	1
Methyl Naphthalenes	7.63+4	0.98	0.99	0.99	0.90	0.21	0.046	3.3	0.76	0.17	8	1
23-Dimethyl Naphth.	1.13+5	0.98	0.98	0.98	1.42	0.38	0.148	5.1	1.36	0.54	5	1
Styrene	8.41+4	0.98	0.99	0.99	0.61	-0.081	-0.32	2.2	-0.30	-1.15	8	10

Table 4 (continued)

Description	kOH [a]	Kinetic Reactivity MIR	MOIR	EBIR	Mech. React'y [b] MIR	MOIR	EBIR	Incr'l. React'y [c] MIR	MOIR	EBIR	Unc. [d]	Doc. [e]
Alcohols and Ethers [g]												
Methanol	1.38+3	0.130	0.20	0.20	2.9	0.93	0.62	0.56	0.28	0.19	1	1
Ethanol	4.81+3	0.38	0.52	0.53	1.7	0.66	0.45	1.34	0.72	0.49	1	11
n-Propyl Alcohol	7.84+3	0.53	0.69	0.69	1.8	0.68	0.45	2.3	1.13	0.74	7	1
Isopropyl Alcohol	7.64+3	0.52	0.68	0.68	0.43	0.19	0.141	0.54	0.32	0.23	7	1
n-Butyl Alcohol	1.22+4	0.68	0.81	0.81	1.5	0.61	0.41	2.7	1.30	0.86	7	1
Isobutyl Alcohol	9.47+3	0.60	0.75	0.75	1.24	0.49	0.32	1.9	0.94	0.63	7	12
t-Butyl Alcohol	1.66+3	0.15	0.23	0.23	1.05	0.41	0.30	0.42	0.25	0.18	7	1
Dimethyl Ether	4.42+3	0.35	0.50	0.50	1.05	0.54	0.43	0.77	0.56	0.45	7	11
Meth. t-Butyl Ether	4.17+3	0.34	0.48	0.48	0.67	0.31	0.24	0.62	0.41	0.31	1	11
Ethyl t-Butyl Ether	1.10+4	0.65	0.79	0.79	1.09	0.46	0.33	2.0	1.03	0.73	7	11
Aldehydes												
Formaldehyde	1.43+4	0.93	0.96	0.96	4.8	1.36	0.71	7.2	2.1	1.09	1	1
Acetaldehyde	2.30+4	0.87	0.93	0.92	2.9	1.07	0.73	5.5	2.2	1.48	4	1
C3 Aldehydes	2.89+4	0.92	0.95	0.95	2.9	1.06	0.70	6.5	2.5	1.6	5	1
Glyoxal	1.67+4	1.00	1.00	1.00	1.34	0.43	0.25	2.2	0.71	0.41	3	1
Methyl Glyoxal	2.52+4	1.00	1.00	1.00	7.4	2.3	1.26	14.8	4.5	2.5	3	1
Ketones												
Acetone	3.39+2	0.051	0.070	0.070	4.5	1.17	0.68	0.56	0.20	0.119	5	1
C4 Ketones	1.70+3	0.19	0.26	0.26	2.4	0.78	0.51	1.18	0.55	0.36	5	1
Aromatic Oxygenates												
Benzaldehyde	1.89+4	0.90	0.98	0.98	-0.20	-0.40	-0.55	-0.57	-1.24	-1.7	5	1
Phenol	3.86+4	1.00	1.00	1.00	0.37	-0.15	-0.35	1.12	-0.47	-1.06	7	1
Alkyl Phenols	6.17+4	1.00	1.00	1.00	0.74	-0.19	-0.51	2.3	-0.58	-1.6	5	1
Others												
Methyl Nitrite	1.76+2	1.00	1.00	1.00	12.1	5.0	4.3	9.5	3.9	3.4	3	13
Base ROG Mixture								3.1	1.17	0.68		

[a] OH radical rate constant as used in the Carter (1990) mechanism in ppm^{-1} min^{-1} units.
[b] Mechanistic reactivities in units of moles carbon per mole C VOC reacted.
[c] Incremental reactivities in units of grams ozone formed per gram VOC emitted.
[d] Notes concerning the uncertainty of the mechanism are as follows:
1 Least uncertain mechanism, and tested against chamber data.
2 Mechanism probably not uncertain, but was not tested.
3 Laboratory data are available for the major reactions in the mechanism, but the mechanism was not tested.
4 Uncertain portions of the mechanism are adjusted or parameterized to fit chamber data.
5 The mechanism is uncertain, and only limited or uncertain data were available to test it.
6 The mechanism was not optimized to fit existing chamber data.
7 The mechanism was estimated and was not tested.
8 The mechanism was estimated and was not tested, and must be considered to be highly uncertain.
9 The mechanism was estimated and was not tested, and is likely to be incorrect. Suitable only for estimating reactivities of mixtures where this is a component.
[e] Documentation notes for the mechanism are as follows:
1 Documented by Carter (1990)
2 Rate constant recommended or tabulated by Atkinson (1989). Parameters calculated using the general procedures discussed by Carter (1990), with updates to the alkyl nitrate yield estimation method as given by Carter and Atkinson (1989b).
3 Parameters and rate constants calculated using the general procedures discussed by Carter (1990), with updates to the alkyl nitrate yield estimation method as given by Carter and Atkinson (1989b).

Table 4 (continued)

4 Mechanism and OH, O_3, and $O(^3P)$ rate constants as documented by Carter (1990). NO_3 rate constants given by Atkinson (1991). If no temperature dependence is given for the NO_3 reaction, the A factor is assumed to be the same as for the OH reaction.
5 Mechanism and rate constants estimated as documented by Carter (1990). NO_3 rate constant estimate updated.
6 Mechanism and rate constants estimated as documented by Carter (1990) except substitutent codes are 2 and 3. NO_3 rate constant estimate updated.
7 Mechanism and rate constants estimated as documented by Carter (1990) except substitutent codes are 3 and 3. NO_3 rate constant estimate updated.
8 Mechanism and rate constants estimated as documented by Carter (1990) except that the method for representing the ozone reactions of cycloalkenes changed so the yield of radicals is the same as for other internal alkenes. NO_3 rate constant estimate updated.
9 OH rate constant as estimated by Atkinson (1989), with the activation energy estimated. The O_3 rate constant was recommended by Atkinson (private communication, 1991), and the NO_3 rate constant was from Atkinson and Aschmann (1988). The Arrhenius A factor for the NO_3 and the O_3 reactions were assumed to be the same as for 1-butene. The $O(^3P)$ rate constant was assumed to be the same as for cis-2-butene, because the OH rate constants are similar. The mechanism is estimated based on assuming all the reaction is at the double bond in a manner analogous to the general alkene mechanism.
10 Rate constant based on values tabulated by Atkinson (1989). The mechanism is highly simplified and used for only qualitative estimates of the contribution of this compound to reactivities of mixtures.
11 The updates to the mechanism is documented by Carter (1991).
12 A new mechanism is used for isobutyl alcohol (2-methyl-1-propanol) since the one in Carter (1990) was in error. The rate constant and relative rates of reaction at the various possible positions were estimated using the method of Atkinson (1987). The mechanisms for the subsequent reactions of the radicals formed were estimated, in a manner generally analogous to the method used for estimating the alkane mechanisms.
13 Absorption cross sections of Calvert and Pitts (1966), with quantum yields of unity assumed for photolysis reaction. OH radical rate constant of Tuazon et al. (1983); see also discussion in Atkinson (1989). Alkoxy radical reactions based on the recommendations of Atkinson (1990).

[f] Reactivities of all alkanes except for methane, ethane, propane, n-butane, n-octane, 224-trimethylpentane, and n-pentadecane calculated using the "pure mechanism species" method as discussed in Appendix B of Carter (1991). This method give results which may be ~5-7% high in some cases.

[g] Reactivities of all alcohols and ethers except for methanol and ethanol were calculated using the "pure mechanism species" method. This method gives results which may be ~5-5% high in some cases.

when NO_x is below MOR levels, the other factors become relatively more important, as indicated by the overlap in the distributions of the mechanistic reactivities in the MOR and EBIR scenarios.

The fundamental chemical process by which VOCs cause ozone formation is the production of HO_2 and other peroxy radicals whose reactions with NO shift the $NO-NO_2-O_3$ photostationary state towards ozone formation. The mechanistic reactivity of CO provides a direct illustration how much ozone is formed by this process, since the only way reaction of CO promotes ozone formation is by forming a single HO_2 radical. From the kinetic differential equations involving O_3 formation and destruction by NO_x, one would expect a maximum of one molecule of ozone to be formed from each molecule of CO which reacts. This theoretical maximum is almost achieved under MIR conditions, with the average MIR mechanistic reactivity for CO being 0.91±0.06. Perfect efficiency of HO_2 formation in forming ozone is not expected since at least some of the ozone so formed would be consumed in other reactions. The formation of ozone from peroxy radicals clearly becomes much less

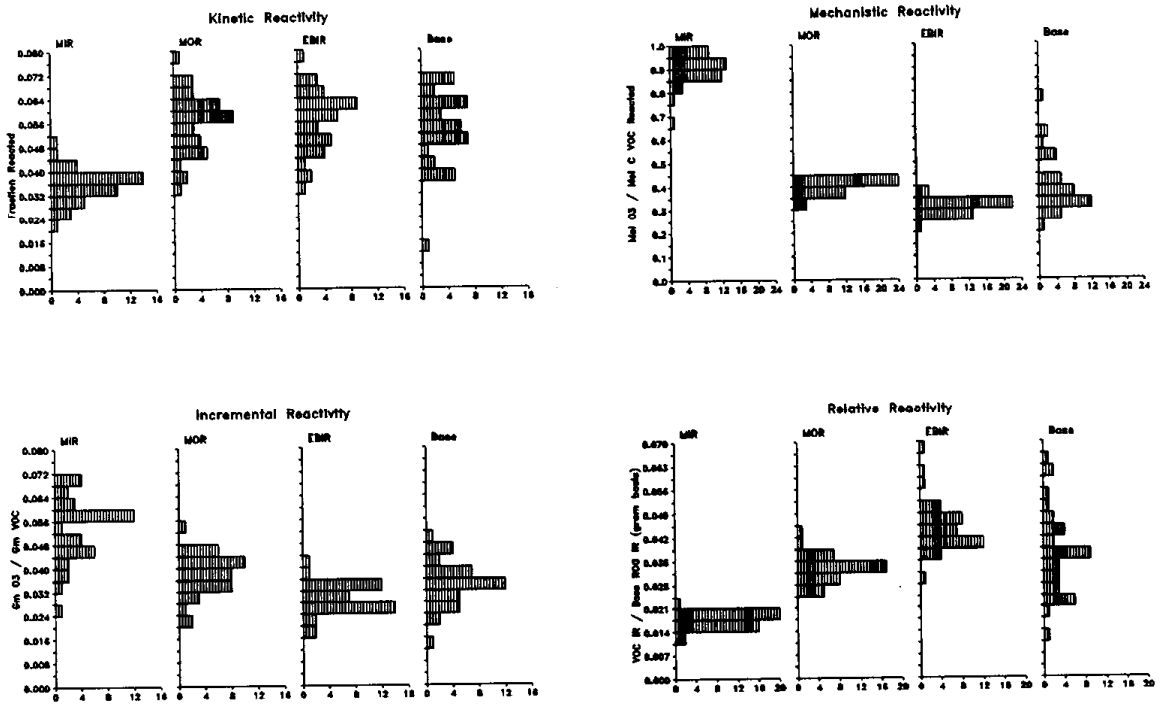

Figure 3. Distribution plots of kinetic, mechanistic, incremental, and relative reactivities of carbon monoxide for the MIR, MOR, EBIR and base case scenarios.

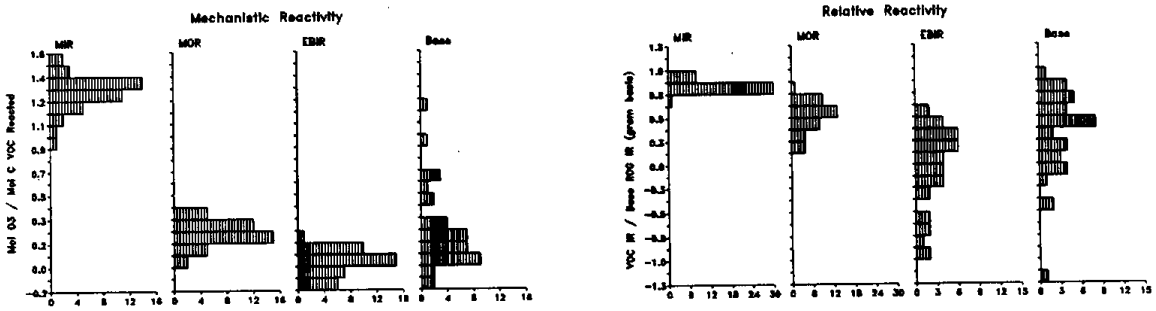

Figure 4. Distribution plots of the mechanistic and relative reactivities of toluene for the MIR, MOR, EBIR and base case scenarios.

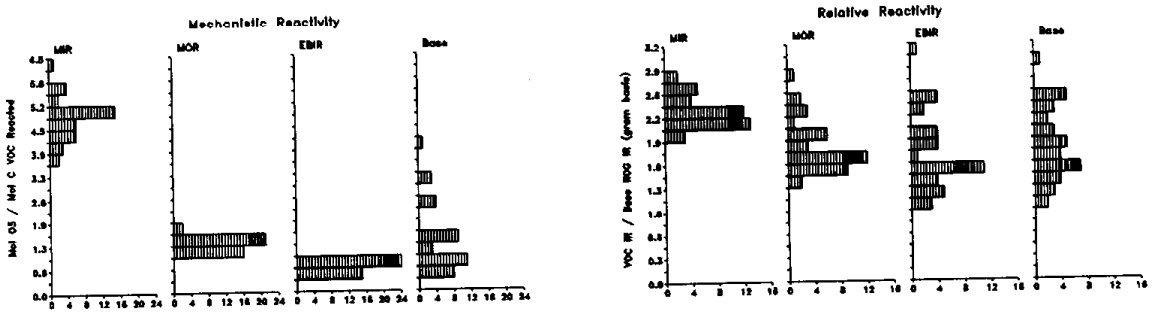

Figure 5. Distribution plots of the mechanistic and relative reactivities of formaldehyde for the MIR, MOR, EBIR and base case scenarios.

efficient at lower NO_x levels, with the mechanistic reactivities of CO being over a factor of ~2 lower under MOR conditions, and by a factor of ~3 lower in the EBIR scenarios. This is because the HO_2+HO_2 reaction, forming H_2O_2, begins to compete with the reaction of HO_2 with NO in the scenarios where all the NO_x is consumed before the end of the simulation. Formation of H_2O_2 is calculated to be a negligible process under MIR conditions, but begins to become important as NO_x is reduced to maximum ozone levels, and increases in importance as NO_x is reduced below that. For example, the H_2O_2 yield in the MIR, MOR, and EBIR averaged conditions scenarios are 0.16, 3.4, and 5.8 ppb, respectively. Formaldehyde and toluene provide examples of compounds whose mechanistic reactivities are significantly influenced by how they effect ozone formation from other VOCs. Formaldehyde and (to a lesser extent) toluene have relatively high MIR mechanistic reactivities because their reactions tend to enhance radical levels, thus causing more of the other VOCs present to react and form ozone. Effects on radical levels are most important under MIR conditions because radical levels determine how rapidly ozone is formed, and the ozone yield is determined by its formation rate. But effects on radicals is also is non-negligible under lower NO_x conditions, as indicated by the fact that formaldehyde also has a high mechanistic reactivity under MOR even EBIR conditions, compared to other VOCs. However, the formaldehyde mechanistic reactivity decreases more rapidly as NO_x decreases than is the case for CO, indicating that effects of radical initiation become less important relative to simple NO conversion as NO_x becomes more limited.

The mechanistic reactivity of toluene becomes low much more rapidly as NO_x is decreased than those for most other VOCs because of the effect of the relatively high NO_x sinks in toluene's mechanism. NO_x sinks become significant when NO_x is limited because it affects the point where NO_x is consumed and ozone

is no longer formed. This becomes the dominant affect when NO_x becomes sufficiently low, causing negative reactivities for VOCs, such as toluene, with sufficiently strong NO_x sinks. This is despite the fact that toluene is still calculated to form radical initiating products and form radicals with react with NO. The crossover for toluene reactivity occurs at some NO_x level around the equal benefit point, though the exact level appears to be highly variable depending on other scenario conditions.

The ways the mechanistic reactivities of the other VOCs are affected by NO_x conditions can be seen from the tabulations of their values for the MIR, MOIR, and EBIR scales on Table 4. In all cases, the mechanistic reactivities decrease monotonically as NO_x is reduced, with the greatest rate of decrease being for compounds which, like toluene, have NO_x sinks in their mechanisms. The phenols and styrene provide the most extreme examples of the latter because these compounds have the strongest NO_x sinks of all the other compounds on the list except for benzaldehyde. Benzaldehyde is unique among the compounds listed in that it has negative reactivities under all conditions. However, the reason for this is not the same under high NO_x conditions as when NO_x is low. Under low NO_x conditions benzaldehyde has negative reactivity because of its NO_x sinks, while under maximum reactivity conditions its reactivity is negative because benzaldehyde is a strong radical inhibitor. Other VOCs, such as the higher alkanes, are also radical and NO_x inhibitors, but in those cases the formation of radicals which enhance ozone by reacting with NO is enough to offset this effect, resulting in these compounds having positive, though small, mechanistic reactivities.

NO_x effects and Variations in Incremental Reactivities.

While the kinetic reactivity is usually the most important single factor in influencing variations of reactivities among different VOCs, the mechanistic reactivity is the dominant factor affecting how the reactivity of a given VOC varies with environmental conditions. In the case of CO and other slowly reacting VOCs, the variability in kinetic reactivities because of variabilities in radical levels among scenarios can be an important factor in affecting variabilities in incremental reactivities, (see Figure 3), but for most other VOCs the variability of the mechanistic reactivities overwhelms any variability in kinetic reactivities. Thus the discussion given in the previous section concerning the variabilities in mechanistic reactivities are also applicable to incremental reactivities.

For most VOCs, the variabilities of the incremental reactivities within the adjusted NO_x scenarios are comparable to the variabilities of the incremental reactivities of the base ROG mixture, which was shown above in Figure 2. (See also Figure 3 for the variability of the incremental reactivities of CO. The

mechanistic reactivity distributions for toluene and formaldehyde on Figures 4 and 5 give a good indication of the incremental reactivity distributions for these compounds.) Typically, the standard deviations of the averages of the incremental reactivities under MIR conditions are ±20-30%, except for compounds, such as the higher alkanes, with very low mechanistic reactivities. The incremental reactivities are somewhat more variable in the MOR and EBIR scenarios, as indicated by the standard deviations of the incremental reactivities of the base ROG mixture, which are 17%, 19%, and 25%, respectively, in the MIR, MOR, and EBIR scenarios. However, the MOR and EBIR reactivities are much more variable for compounds, such as aromatics, with significant NO_x sinks. For example, the incremental reactivities of toluene is negative in some EBIR scenarios, and positive in others.

Contributions to the Reactivity of the Base ROG Mixture.

Since the base ROG mixture is used as the standard to define relative reactivities, it is useful to examine the contributions of the different classes of VOCs to the incremental reactivity of this mixture before discussing relative reactivities. This is summarized on Table 3, above, which gives the percentage distributions of carbons emitted, carbons reacted, and contributions to incremental reactivity of the alkane, alkene, aromatic, and oxygenate components of the base ROG mixture used in the scenarios. (The "carbon reacted" column depends on the kinetic reactivities which as discussed above are somewhat different in the MIR than the other two scales. However, these differences have relatively little effect on the total contributions of the major VOC classes to carbon reacted, so only a single average distribution is shown.)

It can be seen that under MOR conditions the alkanes, alkenes, and aromatics have approximate equal contributions of ~30% to the total incremental reactivity, with the remaining ~10% being due to the oxygenates. The relative contributions of the alkenes and oxygenates remains approximately the same as NO_x is varied, but the contribution of the alkanes increases at the expense of the aromatic contribution as the NO_x levels change from MIR to EBIR conditions. However, this change in relative contributions over this range of NO_x conditions is not dramatic, and it is probably not too rough an approximation to state that the alkanes, alkenes, and aromatics contribute roughly equally to the incremental reactivity of the base ROG mixture under most conditions of interest, with the oxygenates having a relatively small contribution. Thus the variability of the relative reactivity of a VOC will depend on the extent to which their variability of incremental reactivities is similar or different from the variability of an aggregate consisting approximately equally of alkanes, alkenes, and aromatics.

It is important not to confuse the contributions of the different VOC classes to incremental reactivities with their contributions to ozone formation.

VOCs cause ozone formation by forming peroxy radicals which oxidize NO, and, as discussed by Jeffries et al (1991), it is possible to apportion the total ozone formed in a scenario to the radicals formed from the various VOCs and their oxidation products, and thus calculate how much ozone formation can be attributed to reactions of each class of VOC. The result is different than contributions to incremental reactivity because this "contribution to ozone formation" analysis does not take into account the effect of the VOC's reactions on ozone formation from the other VOCs. For example, most of the additional ozone formed when formaldehyde is added to the emissions is not the ozone formed by reactions of radicals produced by formaldehyde, but is the ozone formed from radicals formed from other VOCs which would not have reacted had the formaldehyde not been added. Although we did not calculate contributions to ozone formation for our scenarios, based on the model calculations presented by Jeffries et al. (1991) and our experimental results (Carter, 1992), we would expect the them to be similar to contributions to amounts of carbon reacted. This is indicated by second column on Table 3. Thus, consistent with the calculations of Jeffries et al (1991), the alkanes are expected to have a much higher contribution to ozone formation than they do to incremental reactivity, with correspondingly lower contributions from the other classes of VOCs. However, since control strategies are concerned with effects of changes of emissions, and incremental reactivities measure these effects, these are the quantities of relevance to control strategy applications.

Comparisons of Relative Reactivities in the MIR, MOIR, and EBIR Scales.

The scenario dependencies and variabilities of incremental reactivities are not, by themselves, of significance to the development of VOC reactivity scales, since in practice relative reactivities are the quantities of interest. In general, one would expect relative reactivities to be much less dependent on scenario conditions than incremental reactivities, at least for variations of scenario conditions which affect reactivities of all VOCs in similar qualitative ways. Thus, while decreasing NO_x levels causes decreased incremental reactivities in all compounds, this effect at least to some extent cancels out when considering relative reactivities.

The distributions of the relative reactivities of carbon monoxide, toluene, and formaldehyde in the various types of scenarios are shown on Figures 3-6, and the relative reactivities of these and other selected VOCs are compared graphically on Figures 6-8. (These figures also show base case and $Int O_3$ and $Int O_3$>90 relative reactivities, which are discussed later.) Figures 9 and 10 show how well or poorly the relative reactivities of a number of different VOCs compare in different scales by plotting the relative reactivities of the VOCs in one scale against those in the other. The position of the points for the VOCs should be compared to the 1:1 line where they would fall they had equal relative reactivities in the two scales. Figure 9 compares the MIR and the MOIR scales,

while figure 10 compares the MOIR and EBIR scales. The error bars on the plots in Figures 6-10 give the standard deviations of the averages of the relative reactivities in adjusted NO_x scenarios, and thus indicate the importance of variabilities in non-NO_x related conditions in the scenarios on these relative reactivities.

The results on Figures 3-10 show clearly that ozone yield relative reactivities can depend significant on scenario conditions. The comparisons for the MIR, MOIR, and EBIR scales show how they depend on NO_x conditions. The trend in relative reactivities with NO_x depends on the VOC. Relative reactivities of the aromatics and other compounds with significant NO_x sinks decrease significantly as NO_x is reduced, with the effect being largest for the cresols and benzaldehyde, the compounds with the strongest NO_x sinks. The higher alkenes apparently have similar balances of factors in affecting reactivity as the base ROG surrogate, since their relative reactivities appear to be almost independent of NO_x, especially in the MIR to MOR regimes. (This is in line with the fact that relative contributions of alkenes to the total reactivity of the ROG surrogate are also very insensitive to NO_x conditions.) The relative reactivities of compounds which have weaker than average NO_x sinks, such as CO, ethene and methanol, tend to increase with decreasing NO_x because their incremental reactivities are less sensitive to NO_x than that for the ROG mixture, which includes a 1/3 contribution from aromatics. In addition, relative reactivities of slowly reacting compounds such as CO and ethane tend to increase with decreasing NO_x because kinetic reactivities, which increase as NO_x is reduced, are relatively more important in affecting reactivities of slowly reacting compounds. Because CO is both slowly reacting and has essentially no NO_x sinks, it provides the most extreme case of a compound whose relative reactivity increases with decreasing NO_x.

The distribution plots on Figures 3-5 and the widths of the error bars (the standard deviations) on Figures 6-10 provide an indication of how other scenario conditions affect relative reactivities. For most VOCs, the MIR relative reactivities are quite insensitive to scenario conditions, with the distributions shown on Figures 3-5 being fairly typical. In general, the sensitivities to scenario conditions increase as the NO_x decreases, with the most extreme cases being the compounds, such as toluene, cresols, and benzaldehyde, with the large NO_x sinks in their mechanisms.

Figure 9 shows the extent to which the relative reactivities of positively reactive compounds in the MIR and MOIR scales correspond to each other. Although these relative reactivities are clearly highly correlated, the MIR scale tends to underpredict the MOIR relative reactivities for CO, the alkanes and the alcohols, and overpredict them for the aromatics, on a fairly consistent basis. On the other hand, Figure 10 shows that, except for toluene the MOIR and EBIR

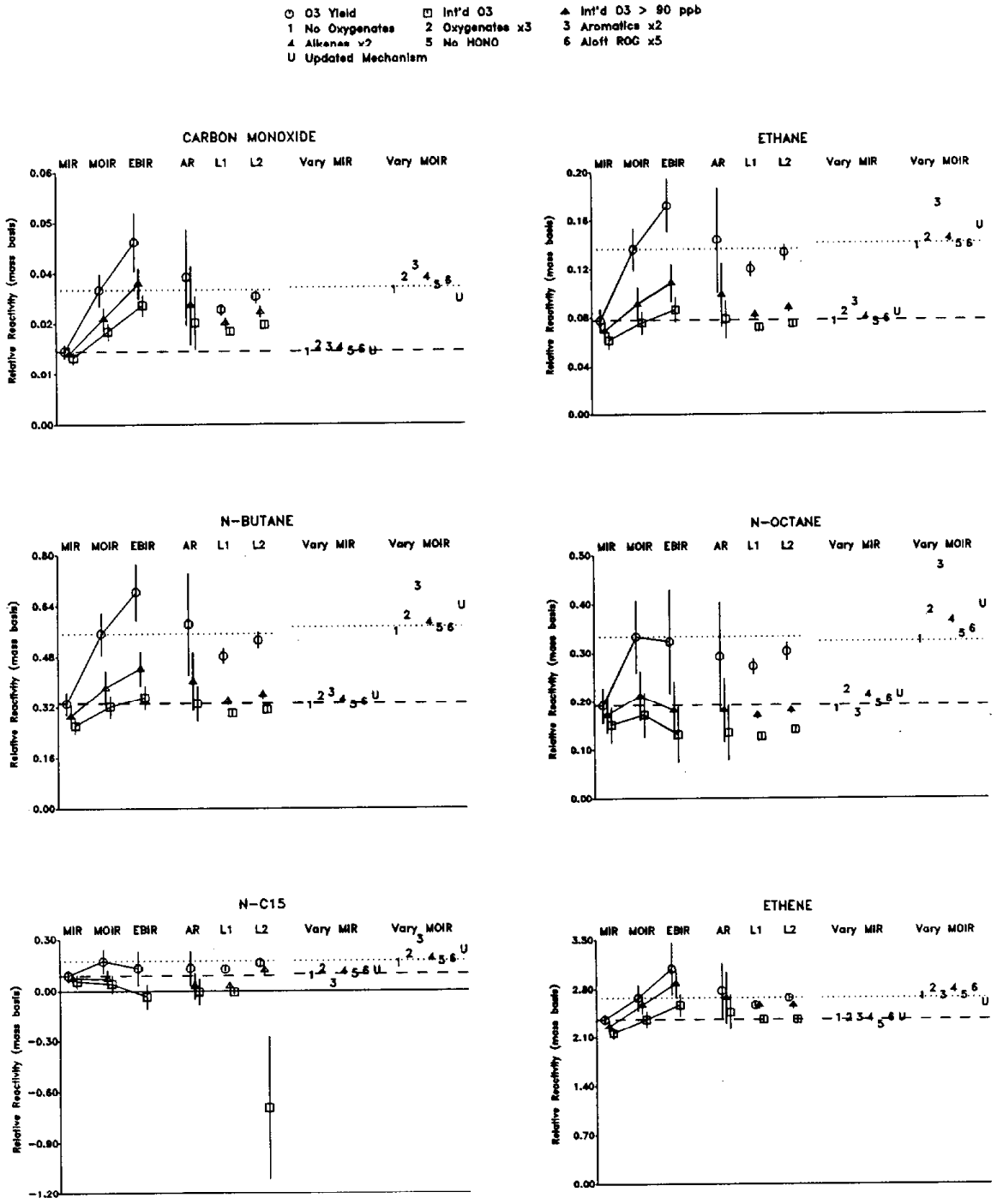

Figure 6. Comparison of relative reactivities of carbon monoxide, ethane, n-butane, n-octane, n-pentadecane, and ethene calculated using various methods. Points on right are ozone yield relative reactivities for the varied averaged conditions scenarios.

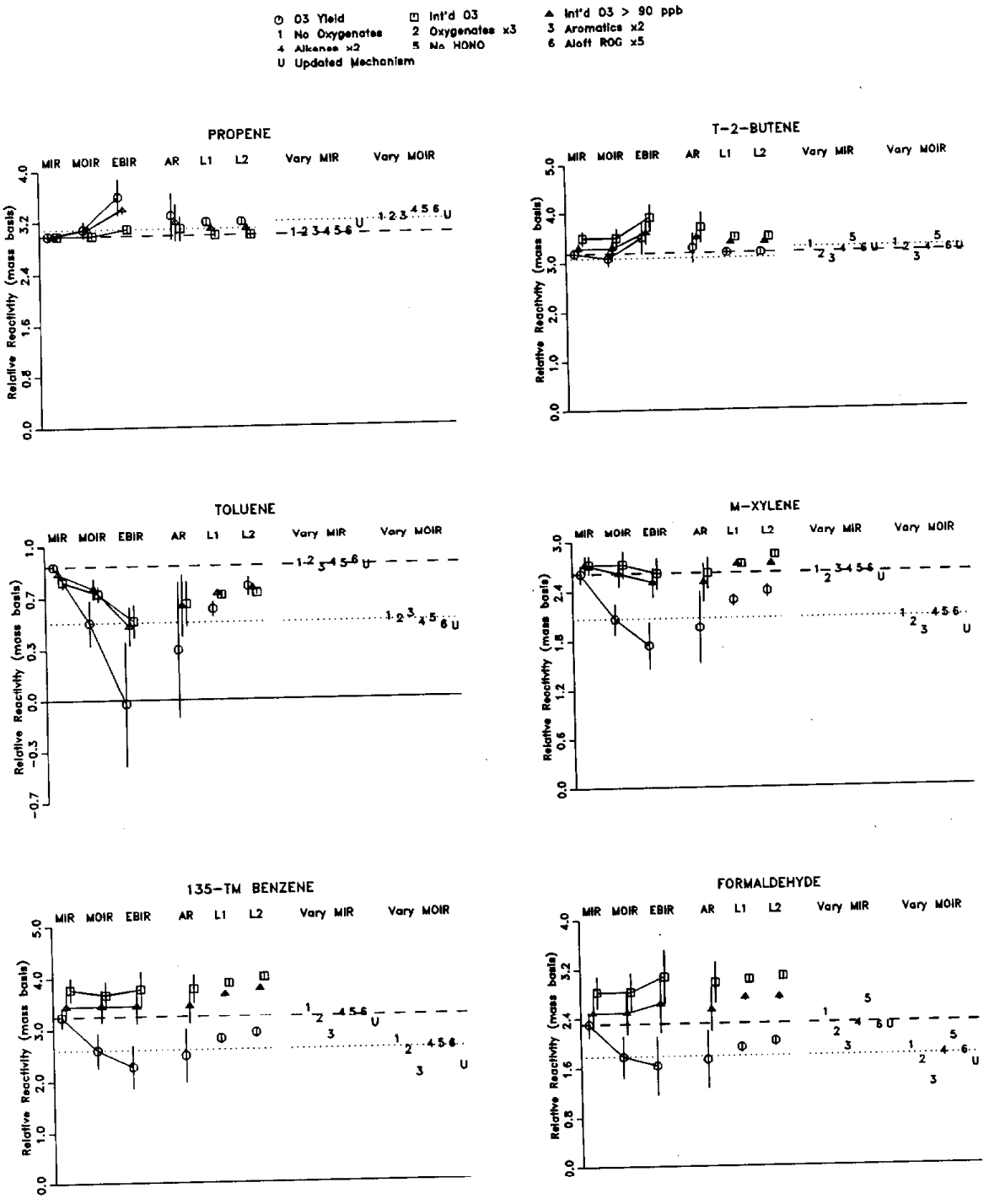

Figure 7. Comparison of relative reactivities of propene, trans-2-butene, toluene, m-xylene, 1,3,5-trimethylbenzene, and formaldehyde calculated using various methods. Points on right are ozone yield relative reactivities for the varied averaged conditions scenarios.

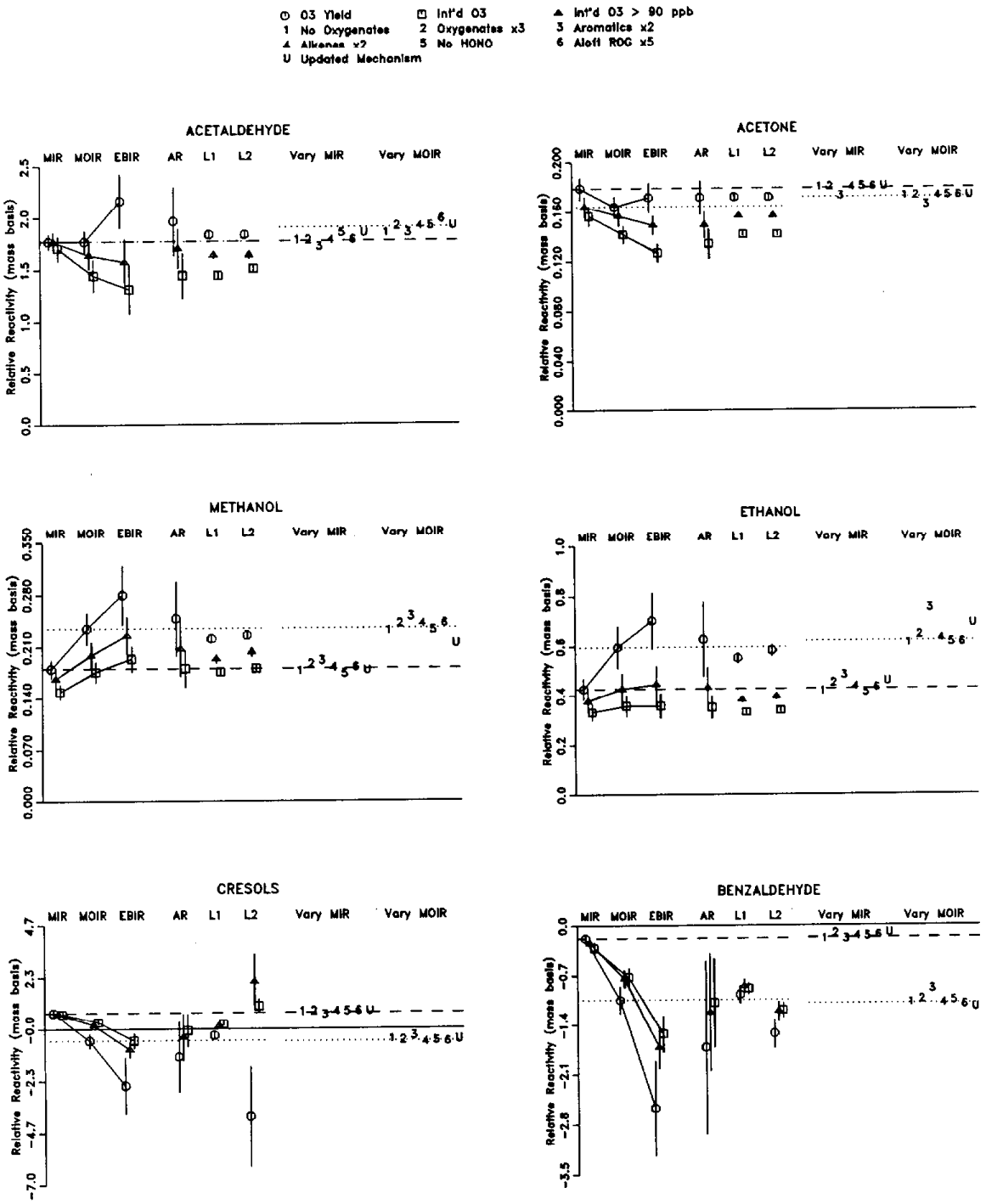

Figure 8. Comparison of relative reactivities of acetaldehyde, acetone, methanol, ethanol, cresols, and benzaldehyde calculated using various methods. Points on right are ozone yield relative reactivities for the varied averaged conditions scenarios.

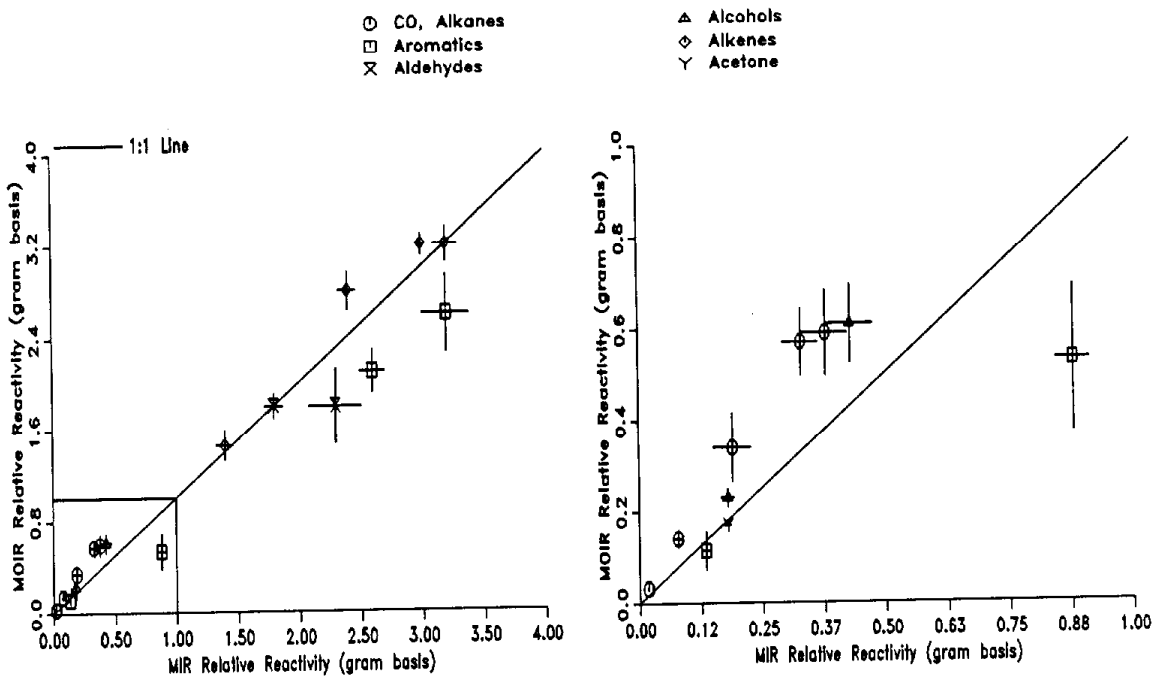

Figure 9. Plots of relative reactivities the MOR scale against relative reactivities in the MIR scale for selected VOCs. The left plot shows the full range of relative reactivities, while the right plot shows the less reactive VOCs more clearly.

relative reactivities correspond very well. These two scales are essentially equivalent to within the uncertainties caused by variabilities in non-NO_x scenario conditions if one considers only compounds which are positively reactive in both scales. These two scales also agree in indicating that phenols and cresols are negatively reactive, while they are positively reactive in the MIR scale. However, the discrepancy in the MIOR and EBIR scales in the relative reactivities of toluene [and by extension the other alkylbenzenes, which the Carter (1990) mechanism assumes have similar reactivities as toluene] is not insignificant in view of the relatively large amounts of these compounds which are emitted.

Base Case Ozone Yield Reactivity Scales.

Figures 6-8 show the various base case ozone yield relative reactivities for the representative VOCs, where they can be compared with those for the adjusted NO_x scales. As before, the "error bars" show the (one σ) standard

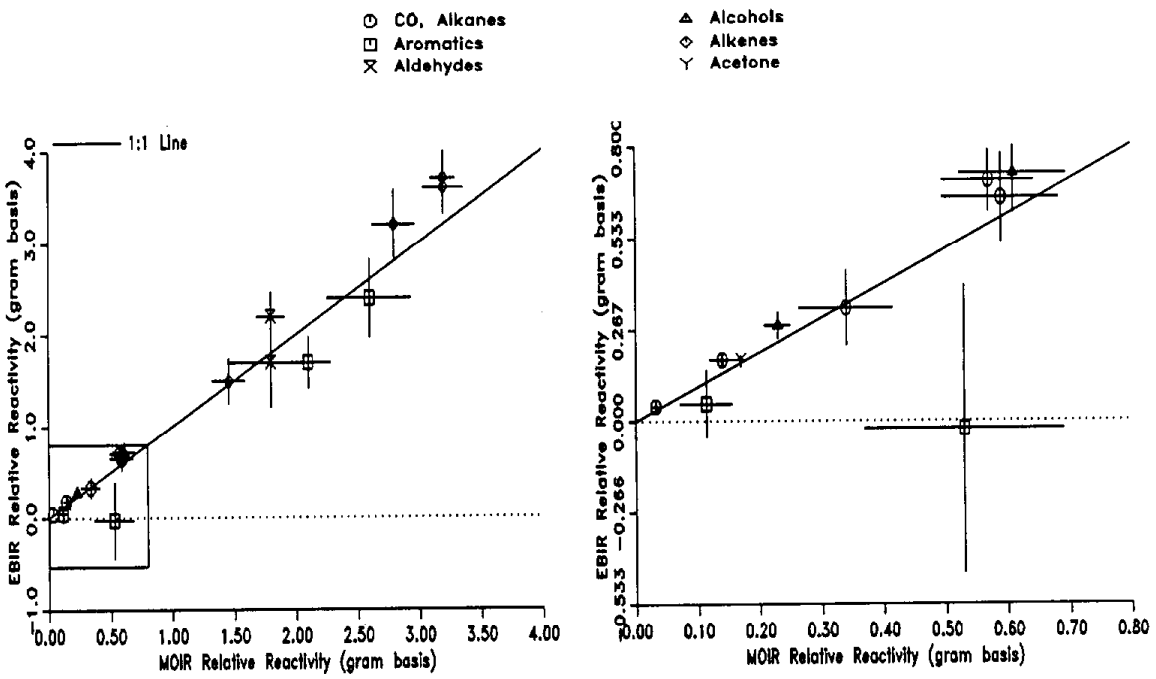

Figure 10. Plots of relative reactivities the EBIR scale against relative reactivities in the MOIR scale for selected VOCs. The left plot shows the full range of relative reactivities, while the right plot shows the less reactive VOCs more clearly.

deviations of the averages or derivations. The average ratio base case [Base(AR)] ozone yield reactivities tend to have high standard deviations because of the variation in relative reactivities in the scenarios due to of the variation of NO_x conditions. However, in most cases the least squares error methods [Base(L1) and Base(L2)] give more well defined values, having standard deviations which are comparable to or smaller than those for the average ratios in the adjusted NO_x scales. There are a few apparently anomalous Base(L2) values which are discussed below.

The Base(AR) relative reactivities in essentially all cases tend to fall somewhere between those in the MOIR and the EBIR scales, being somewhat closer to MOIR than EBIR. This is as one would predict from the distribution of NO_x/NO_x^{MOR} ratios in the base case scenarios. On the other hand, all of the Base(L1) and most of the Base(L2) relative reactivities lie somewhere between the MIR and MOIR values. More MIR-like values for these scales is expected because the least squares error methods put more weight on reactivities in scenarios where ozone is more sensitive to VOCs, i.e., to scenarios which are closer to MIR

conditions. However, unlike the least squares error scale given by Carter (1991), where the Base(L1) scale corresponded much better to the MIR scale than MOIR, in this case the Base(L1) reactivities correspond better to the MOIR scale.

The reason for the differences between this result and those of Carter (1991) arises from the fact that the scenarios employed in the previous study represented a more varied set of NO_x conditions. This is apparent from the distribution plots of NO_x/NO_x^{MOR} ratios on Figure 2, which include the distributions for the Carter (1991) base case scenarios, where they can be compared with the distribution for the EPA base case scenarios used in this study. Although both sets of scenarios have average NO_x/NO_x^{MOR} ratios near the MOR range, the much wider distribution of NO_x conditions in the Carter (1991) scenarios results in a larger fraction of scenarios which have near-MIR or higher-than-MIR NO_x conditions. For example, if we use $NO_x/NO_x^{MOR} \geq 1.3$ as the criterion for defining a near-MIR or higher-NO_x-than-MIR scenario, we find that ~35% of the 1991 scenarios fall into this category, as opposed to only ~4% of these EPA scenarios. Since reactivities in these high NO_x scenarios are weighed the most heavily in computing the least squares error scales, these scales are highly sensitive to the number of high NO_x scenarios in the distribution. There are a sufficient number of high-NO_x scenarios in the 1991 set to dominate the least squares error analyses, yielding relative reactivities which are close to MIR. This is despite the fact that the Carter (1991) scenarios also include a significantly higher fraction of very low NO_x scenarios than in this EPA set. In general, the wider the distribution of NO_x conditions in a set of scenarios, the closer the least squares error reactivity scale derived from it will correspond to an MIR scale.

For most VOCs, the Base(L2) relative reactivities are essentially the same as the Base(L1) values. Thus, as one might expect, the "optimum" reactivity scale when assessing substitutions involving replacing current emissions with emissions of a less reactive VOC is essentially the same as one optimized for assessing substitutions of highly reactive VOCs for increased emissions of all ROGs. However, as can be seen from the data for the cresols and for the n-pentadecane in the integrated ozone case, occasionally apparently anomalous values with high standard deviations, which are outside the uncertainty ranges of the average ratio method, are obtained. These are cases when the incremental reactivities of the VOC are distributed around zero, when the solution of Equation (VII) is most sensitive to the most extreme values in the distribution. Because of the failure of this method in these cases, and the fact that when it does not fail it yields essentially the same result as the L1 method, it is concluded that the L1 method is the clearly preferable method to derive least squares error relative reactivities. This is despite the fact that the L2 method is strictly speaking the more appropriate approach for most of the VOC substitution strategies of current interest, such as alternative fuel use.

Integrated Ozone Reactivity Scales.

The above discussion concerned the reactivities of the VOCs calculated from their effects on the maximum amounts of ozone formed, or ozone yield reactivities. Figures 6-8 also show relative reactivities derived from the effects of the selected VOCs on integrated ozone concentrations (the $Int O_3$ scales) and from the effects of the VOCs on integrated ozone above 90 ppb ($Int O_3$>90), where they can be compared with the ozone yield reactivities discussed above. Both adjusted NO_x and base case results are shown.

The results show that for most VOCs the $Int O_3$ and $Int O_3$>90 reactivities are much less sensitive to NO_x conditions than ozone yield reactivities, and that they tend to correspond much closer to ozone yield in MIR scale than those calculated for lower NO_x conditions. The relative $Int O_3$ reactivities still increase with decreasing NO_x for slowly reacting compounds, and still decrease with decreasing NO_x for the compounds with very strong NO_x sinks, but the change in relative reactivities as NO_x is changed is much less marked is the case for the O_3 yield reactivities. In the cases of a number of the most reactive compounds, such as formaldehyde, m-xylene and trimethylbenzene, the $Int O_3$ reactivities are essentially independent of NO_x, despite the fact that the NO_x dependencies in the ozone yield relative reactivities are significant.

This lower sensitivity of $Int O_3$ reactivities to NO_x conditions means that they have much less variability in the base case scenarios. Because of this the base case relative reactivities are much less sensitive to the method used to derive them, except for the few anomalous Base(L2) cases discussed above.

In general $Int O_3$ reactivities tend to correspond fairly closely to MIR reactivities, even when derived from scenarios with much lower NO_x availability. This is because integrated ozone levels are highly sensitive to how rapidly ozone is formed, even for the lower NO_x scenarios where the final ozone yields are not strongly affected by ozone formation rates. Since the same mechanistic factors tend to be important in affecting rates of ozone formation under all NO_x conditions, the result is that ratios of $Int O_3$ reactivities tend to be less sensitive to NO_x. On the other hand, ozone yields are sensitive to ozone formation rates only high NO_x, near-MIR conditions; under lower NO_x conditions they tend to be more sensitive to factors affecting rates of NO_x availability. While NO_x availability has some influence on integrated ozone levels under low NO_x conditions, it is much less important a factor than the amount of time that the highest levels of ozone were present in the scenario. Thus, $Int O_3$ reactivities are like MIR reactivities because they are both sensitive to aspects of the VOCs' mechanisms affecting ozone formation rates. NO_x sinks in the VOCs' mechanisms, which become the dominant factor affecting MOIR and EBIR reactivities, are only of secondary importance in affecting integrated ozone levels.

One would expect the $Int O_3$>90 reactivity scales to have characteristics somewhere between those for the $Int O_3$ and the ozone yield scales, and this is indeed what is observed. However, the $Int O_3$>90 scales are much closer to $Int O_3$ scales than the ozone yield scales, and all the discussion above for the $Int O_3$ scales are equally applicable to $Int O_3$>90. There are a few cases, such as formaldehyde, trimethylbenzenes, and (to a lesser extent) acetone, ethanol, and methanol, where there is a non-negligible difference between the ozone yield and the integrated ozone reactivities under maximum reactivity conditions. In those cases, the $Int O_3$>90 reactivities tend to be closer to the MIR reactivities.

Because of this, MIR reactivities tend to give very good predictions of $Int O_3$>90 reactivities in the base case scenarios. This is shown on Figure 11, which gives plots of base case $Int O_3$>90 relative reactivities computed using the average ratio method against the values predicted by the MIR scale for selected representative positively reactive VOCs. It can be seen that agreement to within the standard deviations are attained for all but two VOCs, and for those the agreement is within 1.5 standard deviations. This is much better than the correspondence of the base case $Int O_3$>90 reactivities with the MOIR or EBIR scales.

Effects of Variations of Other Scenario Conditions.

The comparisons of reactivities in the adjusted NO_x scenarios provide direct information on their dependencies on NO_x availabilities, and also, through the standard deviations of the averages, provide indirect information on the importance of other conditions which were variable in the scenarios. However, the composition of the base ROG mixture, the level and compositions of ROGs aloft, and the initial nitrous acid (HONO) as a fraction of the NO_x inputs were held fixed in all these scenarios, and thus these data provide no information on the sensitivities of reactivities to these inputs. To asses this, modified versions of the averaged conditions scenario were derived by varying these inputs as described below, then the NO_x inputs for each version were adjusted to derive corresponding MIR, MOR and EBIR scenarios, and then these were used to assess how these variations affect the MIR, MOR and EBIR reactivities.

Four different modifications of the composition of the base ROG were examined, all involving relatively extreme changes to this mixture. These involved only changes to the ROGs associated with anthropogenic emissions, a fraction of which (~60%) were present initially and the remainder emitted throughout the day. The compositions and amounts aloft and biogenic ROGs input were not varied. The variations, and the code numbers used to designate them, are as follows: (1) "No Oxygenates". The aldehydes and ketones were removed without modifying the levels of the other components. (2) "Oxygenates x3". The

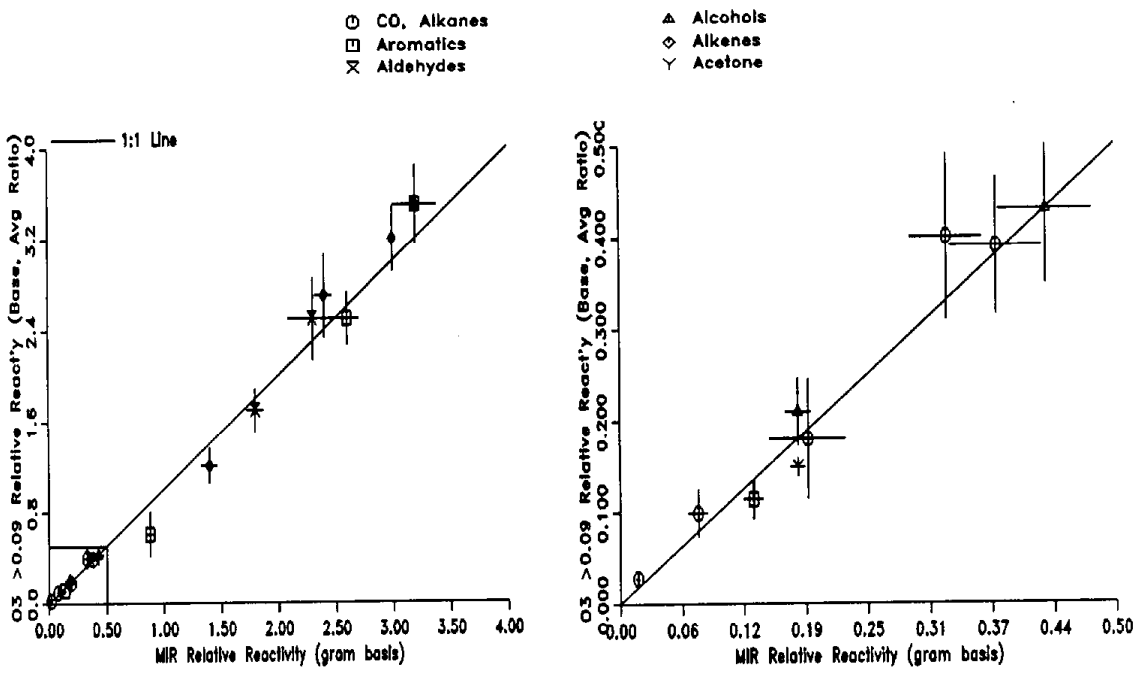

Figure 11. Plots of relative reactivities the Base(L1), IntO_3>90 scale against relative reactivities in the MIR scale for selected VOCs. The left plot shows the full range of relative reactivities, while the right plot shows the less reactive VOCs more clearly.

aldehydes and ketones were increased by a factor of 3 without modifying the levels of the other components. (3) "Aromatics x2". The aromatics were increased by a factor of 2, and the alkanes and olefins reduced to keep the total carbon the same. (4) "Alkenes x2". The olefins were increased by a factor of 2 and the alkanes and aromatics reduced to keep the total carbon the same.

One of the changes made to the EPA scenarios was assuming that ~2% of the initial NO_x was in the form of nitrous acid (HONO), which is a powerful photoinitiator which could help initiate the photochemical processes early in the day. The EPA scenarios as received from Bauges (1991), and the scenarios used previously (Carter, 1991), assumed no initial HONO. The (5) "No HONO" modification, where the initial nitrous acid (HONO) was assumed to be zero and no HONO was subsequently emitted, was used to assess the effect of this change.

The scenarios as received from Bauges all assumed a standard 30 ppb of VOCs aloft, and this was not modified in the calculations discussed above. The same

chemical composition was also used for this aloft mixture in all scenarios. The (6) "Aloft ROGs x5" modification, where the concentrations of all ROGs aloft were increased by a factor of 5, was used to assess how important aloft ROGs are in affecting reactivity calculations in these scenarios.

The MIR and MOIR relative reactivities calculated using these modified scenarios are shown for the representative VOCs on the right hand side of the plots on Figures 6-8, where they can be compared with the values for the corresponding averaged conditions scenario. The relative reactivities in the varied scenarios are indicated by the code numbers on the plots, while the standard, or averaged conditions, values are indicated by the dashed (for MIR) or dotted (for MOIR) lines.

The data on Figures 6-8 show that these relatively large variations in the base ROG mixture had in most cases had only small effects on the relative reactivities. The variation which had the largest effect was the increase in the aromatics ("3" on the plots), whose twofold increase, for example, caused a ~19% decrease in the relative MIR reactivity of formaldehyde. Removing the oxygenates from the base ROG ("1") increased the relative MIR reactivity of formaldehyde by only ~7%, in contrast with the results with the scenarios of Carter (1991) where a larger effect (though on incremental rather than relative reactivity) was noted. The effects of these variations on the other VOCs were generally smaller, except for VOCs, such as n-pentadecane, which are highly sensitive to almost all variations.

The removal of initial HONO from the scenarios ("5") had almost no effect on any of the results except for formaldehyde, whose MIR and MOIR relative reactivities increased by ~15%, and whose integrated ozone relative reactivities (not shown) increased by ~20%. This is a large sensitivity in view of the almost complete insensitivities of the other results to initial HONO. Since both HONO and formaldehyde provide early radical sources in the simulations, this shows that removing one such radical source increases the sensitivity of the scenarios to the other.

The fact that these scenarios have initial HONO while those of Carter (1991) do might partly explain why the formaldehyde reactivity in these scenarios is less sensitive to changes in aldehyde emissions than calculated previously. In the absence of the initial HONO, we calculate that the relative reactivity of formaldehyde increases by ~11% when the base ROG oxygenates are removed. (This is not shown on the plots.) This is greater than the ~7% effect observed when the HONO is present, and indicates that adding radical initiators such as HONO to the scenario reduces the sensitivity of formaldehyde reactivities on initial aldehydes.

The fivefold increase in the aloft ROGs was found to have an insignificant affect on the relative reactivity results. In view of this, the sensitivity to the composition of the aloft ROG mixture would also be expected to be small.

Effects of Mechanism Updates.

Another input which was held constant in all the simulations discussed above was the chemical mechanism. Like all mechanisms used in current airshed models (e.g., Stockwell et al, 1990, Gery et al, 1988), the Carter (1990, 1991) mechanism used in this work is also out of date in some respects (Gery, 1991). For example, the Carter (1990) mechanism uses somewhat lower absorption cross sections for formaldehyde than indicated by the data of Cantrell et al. (1990) and Rogers (1989), and the data of Tuazon et al. (1991) and Bridier et al. (1991) indicate that the acetyl peroxy + NO_x rate constants need to be changed such that the rate of formation of PAN when $[NO]=[NO_2]$ would be decreased by ~40%. We had developed a version of this mechanism which included these updates and intended to utilize it when calculating the MIR scale for the CARB. However, when this was re-evaluated against the chamber data using the methodology of Carter and Lurmann (1991), the ~15% bias in overpredicting ozone observed when the Carter (1990) mechanism simulated complex mixtures increased to ~24% (Carter, unpublished results). This is due primarily to the effect of the change of the peroxy acetyl radical kinetics. This ~24% bias was judged to be unacceptable. Because of this, the decision was made not to utilize this mechanism to calculate reactivity scales until we have had a chance to re-examine and update the data base and methodology used to evaluate the mechanism against the chamber data, and to utilize this updated data base when making any necessary adjustments to the various uncertain parts of the mechanism. This effort is underway now.

Although the updates concerning the peroxy acetyl radical kinetics and (to a lesser extent) formaldehyde photolysis had non-negligible effects on simulations of ozone yields, it is less clear whether they would significantly affect predictions of relative reactivities. To assess this, the updated mechanism was used to calculate relative reactivities of selected VOCs in the averaged conditions scenarios under the various NO_x conditions. The results are shown on Figures 6-8, with the other "Vary MIR" and "Vary MOIR" points, using the "U" symbols. (The results for EBIR conditions are similar to those for MOR, though the sensitivity is somewhat greater.) The change in the mechanism caused less than a 10%, 15%, or 20% change in MIR, MOIR, or EBIR relative reactivities, respectively, except for VOCs with very low or negative mechanistic reactivities. Perhaps surprisingly, the relative reactivities of formaldehyde and acetaldehyde, the two compounds one would expect to be most affected by these changes, were no more sensitive to these changes than those for the other VOCs. Therefore, at

least these updates do not appear to have a substantial effect on relative reactivities for major VOCs which contribute to ozone formation.

Examples of Exhaust Reactivity Adjustment Factors.

An example of a regulatory application of a reactivity scale is the utilization of reactivity adjustment factors (RAFs) in the alternative fuel vehicle exhaust standards recently adopted in California (CARB, 1990). The mass emissions of exhausts from alternatively fueled vehicles are multiplied by these RAFs to place them on the same ozone impact basis as emissions from conventional vehicles. They are calculated from the ratios of incremental reactivities (as ozone per gram) for the exhaust mixtures from alternative fueled vehicles, relative to that for an exhaust mixture characteristic of conventionally fueled vehicles. Although the regulation as adopted utilizes the MIR scale to calculate these RAFs, it is of interest to see how these would differ if other scales were used. This is shown on Figure 12, which gives RAFs for selected vehicle exhaust mixtures calculated using the various reactivity scales. The example mixtures, which are based on analysis provided by the CARB (1991), include exhausts from vehicles fueled with 85% methanol + 15% gasoline (M85), condensed natural gas (CNG), liquified petroleum gas (LPC), and 85% ethanol + 15% gasoline (E85). The RAFs are calculated relative to the standard exhaust mixture used by the CARB (1991).

The format for the data on Figure 12 is similar to that on Figures 6-8. The MIR, MOIR, EBIR and Base(AR) RAF's are the average of ratios the RAFs in the various types of scenarios, calculated from ozone yield, $IntO_3$ and $IntO_3>90$ incremental reactivities. The LSE RAF's shown are those which give the minimum the least squares error in ozone yield, integrated O_3, or integrated $O_3>90$ ppb in the null tests where the alternative fuel exhaust is substituted for the standard exhaust. They are calculated in a manner analogous to the Base(L2) method except that the reactivity of the standard exhaust is used in place of that for the base ROG. The points under "Vary MIR" and Vary MOIR" show the effects of varying the various scenario conditions or using the updated mechanism on the MIR or MOIR RAFs, in manner analogous the variations discussed in the previous two sections.

For all four exhausts the RAFs tend to increase with decreasing NO_x conditions, except that the integrated O_3 RAFs for E85 are almost independent of NO_x. The M85 RAF is least sensitive to the scale used, but is somewhat unique in that the integrated ozone and ozone yield RAFs have about the same dependence on NO_x. The RAFs for the other mixtures are more typical of relative reactivities in general in that the integrated O_3 RAFs are less sensitive to NO_x than ozone yield values. The fact that the MIR scale predicts the lowest RAF in all

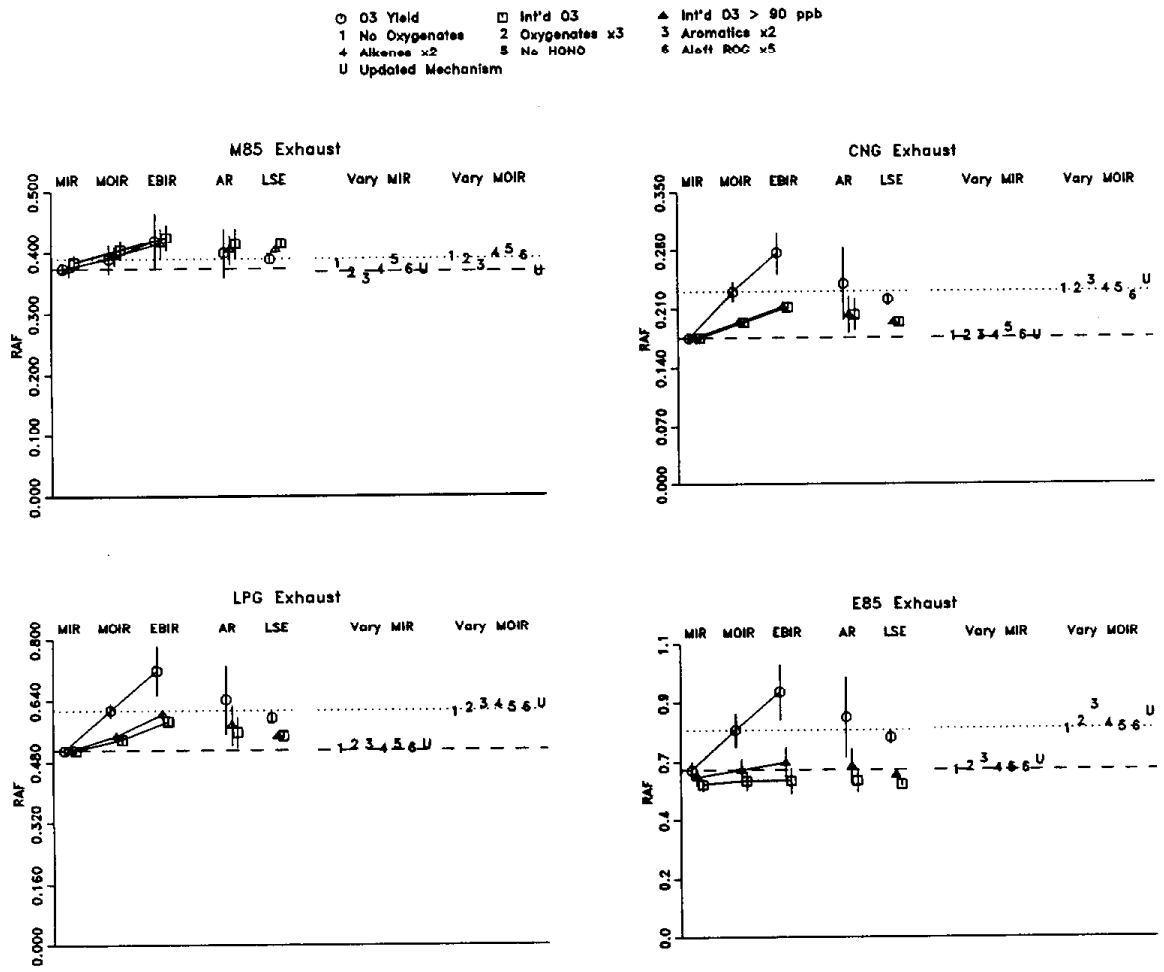

Figure 12. Comparisons of Reactivity Adjustment Factors for selected vehicle exhaust mixtures calculated using various methods. Points on right are calculated from ozone yield RAFs for the varied averaged conditions scenarios.

cases (except E85) might suggest that the MIR has a bias towards giving undue credits to alternative fuels. This increase in RAF with decreasing NO_x is due to the fact that alternative exhausts have more slowly reacting compounds whose reactivities are affected by the lower radical levels in MIR scenarios, and by the fact that the alternative exhausts tend to have less species with strong NO_x sinks (e.g., aromatics) than the standard exhausts. However, regardless of this variability, the range of RAFs do not overlap unity except for E85.

The points on the right hand side of the plots show that the variations in the base ROG mixture, the removal of initial HONO, and the increase in aloft ROGs

will not significantly affect the RAFs in these cases. Using the updated mechanism has essentially no effect on the MIR RAFs and only a slight effect on the MOIR values. Thus the main issue in affecting RAFs do not relate to these uncertainties, but to what type of scale is most appropriate.

Appropriate Reactivity Scale for Regulatory Applications.

The dependence of relative reactivities environmental conditions means that different reactivity scales will give different predictions of effects of proposed VOC substitutions. Because of this, it clearly best not to use reactivity scales, but instead base regulatory decisions on comprehensive assessments of effects of the proposed strategies on the full range of relevant airshed conditions. However, this approach is not practical in all circumstances. In cases where comprehensive analyses or use of multiple scales in not practical, the options remaining are either ignoring reactivity altogether or using a scale which gives at least give some indication of relative ozone impacts.

The first question is whether ignoring reactivity altogether is the better option. This is equivalent to adopting a scale where all non-exempt VOCs have a relative reactivity of 1. Adopting such a "scale" might be appropriate if reactivities were so variable in different scenarios that they could be considered to be the same to within this variability. The results of this study do not support this conclusion. Although there are differences in relative reactivities among the scales, in most cases these differences are small compared to the wide range of relative reactivities of the VOCs. For example, both propane and formaldehyde are currently regulated as ozone precursors, yet formaldehyde is 10 to 30 times more reactive than propane in all the 18 scales derived in this work. Thus, while there is a factor of 3 variability in the relative reactivities of these compounds over the full range of relevant conditions, this is still significantly less than the factor of 10 minimum difference between them. Note also that of the 18 different types of VOCs shown on Figures 7-9, only one (cresols) have reactivity scales whose uncertainty ranges overlap 1. The relative reactivities for 10 are always less than 1 and those for the other 7 are always greater than 1. Thus, even if one accepts the proposition that relative reactivities under highly NO_x-limited conditions such as EBIR should be given equal weight as MIR reactivities, there still would be many clear cases where some VOCs are unambiguously more reactive than others, and thus where ignoring their reactivity difference would be inappropriate.

The question then is which of the various possible scales is the most appropriate to use in applications requiring a single scale. Although we derived a total of 18 scales in this work, there are actually only three types of scales

if we consider their major features. These are: (1) scales which are sensitive to the effect of the VOC on ozone formation rates; (2) scales which reflect the effect of the VOC on ozone yields under conditions which are most favorable for ozone formation; and (3) scales which reflect the effect of the VOC on ozone yields under highly NO_x-limited conditions, of which the EBIR is the only example derived in this work. The scales in the first category are the MIR and the integrated ozone scales. The scales in the second category include the MOIR scale and (for these EPA scenarios) the base case ozone yield scales. These are referred to as "MIR-like" and "MOIR-like", respectively, the subsequent discussion. The only representative of the third category derived in this work is the EBIR scale. The EBIR scale (which in many respects MOIR-like except for toluene and other NO_x-sink compounds) is clearly not optimum because it reflects conditions where ozone is relatively insensitive to VOCs and because it resembles none of the base case scales. Thus the real choice is between MIR-like or MOIR-like scales.

The MOIR scale is attractive because it is based on an atmospheric condition which is clearly a better approximation of the base case scenarios used in this work than MIR. For this reason, the average ratio ozone yield reactivity scale corresponded to the MOIR scale. In addition, there were so few of these EPA-developed base case scenarios which were near MIR conditions that even the least-squares error ozone yield scales, which weigh reactivities in the MIR-like scenarios most heavily, resembled the MOIR scale. Thus, if the policy is adopted that regulations should focus on effects of VOCs on peak ozone levels under worst-case or near-worst case conditions, and if it is assumed that the distribution of NO_x conditions in the EPA scenarios is an appropriate representation of those conditions, then an MOIR-like scale would be the most appropriate one to adopt.

However, the fact that so few of the base case EPA scenarios are near MIR conditions does not imply that such conditions rarely occur in the atmosphere. Each of these scenarios are based on the EPA's assessment of the conditions of a near-worst ozone episode in some area. Therefore, each represents a meteorological condition which is near to the most favorable for ozone formation that occurs in that area. Thus most other days would have less favorable meteorological conditions for ozone, including those where unacceptable ozone levels are still formed. Many of these would include days with lower rates of NO_x removal because lower temperatures or light intensities cause lower rates of photochemical reactions. If NO_x is removed more slowly, then lower amounts of NO_x are required to achieve a given level of NO_x availability. This means that if NO_x emissions are held constant the NO_x availability will be greater, i.e., the scenario would become closer to MIR conditions. As indicated above, ozone can still exceed air quality standards under MIR conditions, so such meteorologi-

cal conditions, while not worst case, are not irrelevant to the problem of urban ozone formation.

Therefore, a distribution of scenarios which included episodes which were not among the worst for the areas would be expected to have relatively more scenarios at or near the MIR range than is the case for these EPA scenarios. If a sufficient number of such scenarios are included, the base case ozone yield scales derived using the least squares error methods would become more MIR-like than MOIR-like. This was observed with the scenarios used in our previous study (Carter, 1991), which represented a much broader distribution of NO_x conditions. Therefore, if one assumes the least squares error method represents an appropriate approach for deriving a multi-scenario reactivity scale, and if the distribution of scenarios included all ozone non-attainment conditions and not just the worst cases, then the resulting base case ozone yield scale might be more like MIR than MOIR. In general, the more variable the conditions being considered, the more likely such a scale would resemble MIR.

The MIR scale is clearly superior to MOIR if one adopts the policy that VOCs should be regulated based on their effects on integrated ozone or integrated ozone above the standard. This is indicated by the close correspondence between the MIR scale and the base case $Int O_3>90$ scale shown on Figure 10. This correspondence is not an artifact of using the EKMA model formulation, since Russell (1990) used the CMU grid model of two Los Angeles episodes to calculate effects of VOC classes on integrated ozone over the California and Federal standards, and found that the resulting relative reactivities were very close to those predicted by the MIR scale.

The CARB chose the MIR scale to calculate the RAFs in the California vehicle regulations based primarily on the following arguments: (1) MIR represents conditions where regulating VOCs are most effective for reducing ozone. (2) Using MIR complements California's NO_x-control strategies, which are most effective for reducing ozone under the NO_x-limited conditions where MIR is least appropriate. (3) The MIR scale gave good predictions of the integrated ozone reactivities calculated by Russell (1990) using a much more complex physical model (Russell et al. 1989). The calculations of Russell (1990) also increased the level of confidence in the validity of the MIR derivation because they showed that a detailed physical model (Russell et al. 1989) with condensed chemistry (Lurmann et al, 1987) can give essentially the same reactivity scale as a simplified physical model with detailed chemistry.

The main reason that scales like MOIR scales are different from those like MIR is that the former tend to give VOCs reactivity credits if they have NO_x sinks in their mechanism, while the latter does not. NO_x sinks in a VOCs mechanism means it forms high yields of nitrogen-containing compounds such as

PAN's, organic nitrates and nitro-compounds when it reacts. Many of these products may be may have significant or at best uncertain toxicity. Although NO_x sinks do reduce ozone under NO_x-limited conditions, it can be questioned whether it is appropriate to adopt policies which encourage use of VOCs which form such potentially toxic nitrogen-containing products.

Although use of an MIR-like scale is probably more appropriate than the other alternatives for regulatory applications requiring a single scale, the MIR scale itself may not necessarily be the best scale for this purpose. As discussed above and shown on Figure 2, MIR conditions are not typical of the distribution of conditions of the types of episodes used to design ozone control strategies. The lower radical levels characteristic of MIR conditions may give undue reactivity credits to slower reacting VOCs such as methanol because such VOCs more sensitive to radical levels. "Null test" airshed model calculations on effects of substitution of the standard exhaust for M85 and LPG suggested that the MIR may be biased towards giving low RAFs (Mc.Nair et al., 1993). Because of this, the CARB applied a 10% upward "correction" to the RAF for M85 before adopting it. Although a 10% correction is small compared considering the variabilities of reactivities with conditions, the potential for a consistent bias in the MIR scale is obviously a concern.

Since the main argument for using MIR centers on the fact that it corresponds well to effects of VOCs on integrated ozone in base case or physically detailed scenarios, it might be more appropriate to use a base case integrated ozone scale rather than MIR for regulatory applications. At least this would eliminate the criticism, often made of MIR, that the scale is based on atypical conditions. It may also address the potential bias problem for calculating low RAFs which seems to be characteristic of MIR for a number of alternative fuel exhausts being considered. For example, the least squares error $Int O_3>90$ RAF for M85 is 0.40, which, though only slightly higher than the MIR value of 0.37, is essentially equivalent to the "corrected" M85 RAF of 0.41 which was adopted by the CARB. Thus, no correction factor would be needed had this scale been used in the first place. As shown on Figure 12, the RAF's for CNG and LPG would also be slightly higher in this scale than in MIR — though the RAF for E85 would be essentially unaffected. However, these are fairly minor adjustments, and, as shown on Figure 11 for all practical purposes the MIR and the base $Int O_3>90$ scales can be considered to be essentially equivalent.

CONCLUSIONS

A quantitative reactivity scale which compares the effects of different types of VOCs on ozone formation could be useful for a number of ozone control strategy applications. However, the development of such a scale has a number of difficulties. These can be categorized into three major areas. The first is that the gas-phase chemical mechanisms by which VOCs react in the atmosphere to form ozone are in many cases highly uncertain. This results in uncertainties in the model predictions a the reactivity of a VOC in any given scenario. The second is that the effects of VOCs on ozone formation – their reactivities – depend on the environment in which they are emitted. This means that even if we are capable of reliability predicting the reactivity of a set of VOCs in a set of scenarios, it is not obvious how these results should be used in developing a single reactivity scale – or even whether a use of a single reactivity scale has any validity. The third is that there are uncertainties in conditions of airsheds and episodes where unacceptable levels of ozone are formed. The uncertainties in conditions of a specific episode affect predictions of VOC reactivities for that episode, and uncertainties in distribution of conditions affect the development of appropriate methods for aggregating scenario-specific reactivities into a generalized reactivity scale.

The focus of this report has been on the second of these problems, that of deriving a reactivity scale given that reactivities depend on environmental conditions. This has been studied by deriving reactivity scales using several different techniques, given a single chemical mechanism and a single set of representative airshed scenarios. The chemical mechanism employed is uncertain for many VOCs, but it incorporates our current best estimate of their atmospheric reactions, and represents most of the major types of species which need to be incorporated in reactivity scales. The representative environmental scenarios employed are even more uncertain, but they represent their developers' best estimate of the conditions of a wide variety of representative pollution episodes given the limitations in available data and the constraints of the simplified physical formulation of model used. This is sufficient for the purpose of at least an initial evaluation of methods for deriving reactivity scales.

Differences in availability of NO_x is the most important reason why VOC reactivities vary from scenario-to-scenario. This is often measured by the ROG/NO_x ratio, though this is not always a good predictor of NO_x availability because of variability of factors affecting rates of NO_x removal. The ratio of NO_x to NO_x levels giving maximum ozone concentrations was found to be a much better measure of this. NO_x conditions yielding maximum incremental reactivity

(MIR), and NO_x conditions where VOC and NO_x reduction are equally effective in reducing ozone (EBIR) represent respectively the high and low limits for conditions of NO_x availability which are relevant for defining a VOC reactivity scale. Therefore comparison of relative reactivities in the MIR and the EBIR scales give an appropriate indication of the effect of uncertainties in relative reactivities due to variations or uncertainties in NO_x conditions.

Consistent with results of previous studies, it was found that the NO_x conditions can significantly affect relative as well as absolute reactivities. In addition, it was also found that relative reactivities can depend on how ozone impacts are quantified, especially under low NO_x conditions. Because of this, different reactivity scales give different reactivity rankings for VOCs and in some cases different orderings of VOCs in these rankings. However, in most cases the qualitative rankings are unambiguous and the differences in rankings among the different scales are small compared to the full range of reactivities of those VOCs which are now regulated as ozone precursors. It is not true that the that reactivities are so strongly dependent on scenario conditions that all VOCs can be considered to be equal to within this variability. Use of some appropriate type of scale will yield more a more efficient ozone control strategy than regulating all VOCs equally – the main issue is what is the optimum type of scale to use and what is its level of uncertainty.

Although a total of 18 different scales based on various NO_x conditions and methods for quantifying ozone were derived, the essential choice is between a scale like MOIR which is based on effects of VOCs on ozone concentrations when NO_x is not in excess or a scale like MIR which is based on the effects of the VOC on ozone formation rates and integrated ozone levels. Although there are valid arguments for each type of scale, it is concluded that if only one scale can be used, a scale like MIR is more appropriate. While the MOIR and scales like it are most effective at addressing peak ozone levels under conditions which are the most favorable for ozone formation, the scales like MIR it are more optimal when applied to the full wide variety of conditions where ozone is sensitive to VOCs, or when one is concerned with reducing exposure to integrated ozone or ozone over the air quality standard.

Although these conclusions are based on reactivities calculated for highly simplified, single day, and perhaps in some cases inaccurate scenarios, the scenarios employed are sufficiently varied that it is not unreasonable to expect that similar results would be obtained if a more detailed and accurate scenarios were employed. However, it is also clear that further work is needed to develop and utilize a more comprehensive and physically realistic set of scenarios for VOC reactivity assessment. All the scenarios used in this work represented the reactions of the VOCs only over a single day, and scenarios involving multi-day episodes and regional models are needed to assess the total impact of VOCs on

ozone over their lifetimes. The work of Russell (1990), who calculated integrated ozone reactivities of lumped model species in physically detailed models of two different three-day Los Angeles episodes, is an important start in this regard. The fact that they obtained essentially the same relative reactivities as expected based on this work gives us increased confidence in the general applicability of these results. However, this needs to be further evaluated using physically detailed models of other areas, and using regional models which can assess the impacts of VOCs over longer time periods and in long range transport scenarios.

It should be recognized that regardless of which approach or set of airshed conditions is used for developing a reactivity scale, model calculations of VOC reactivities are no more reliable than the chemical mechanism used to calculate them. Modeling studies may give us an indication of the magnitudes of the effects of these uncertainties, but will not reduce them. To reduce these uncertainties, experimental data are needed to test the mechanisms used to derive the reactivity factors, or at a minimum to test their predictions of maximum reactivity. Such experiments are underway in our laboratories.

REFERENCES

Altshuller, A. P., and J. J. Bufalini (1971): Environ. Sci. Technol. 5, 39, and references therein.

Atkinson, R. (1987): "A Structure-Activity Relationship for the Estimation of Rate Constants for the Gas-Phase Reactions of OH Radicals with Organic Compounds," Int. J. Chem. Kinet., 19, 799-828.

Atkinson, R. (1989): "Kinetics and Mechanisms of the Gas-Phase Reactions of the Hydroxyl Radical with Organic Compounds," J. Phys. Chem. Ref. Data, Monograph No. 1.

Atkinson, R. and S. M. Aschmann (1988): Int. J. Chem. Kinet. 20, 513.

Atkinson, R. (1990): "Gas-Phase Tropospheric Chemistry of Organic Compounds: A Review," Atmos. Environ., 24A, 1-24.

Atkinson, R. (1991): "Kinetics and Mechanisms of the Gas-Phase Reactions of the NO_3 Radical with Organic Compounds," J. Phys. Chem. Ref. Data, 20, 459-507.

Bauges, K. (1990): "Preliminary Planning Information for Updating the Ozone Regulatory Impact Analysis Version of EKMA," Draft document, Source Receptor Analysis Branch, Technical Support Division, U. S. Environmental Protection Agency, Research Triangle Park, NC, January.

Bauges, K. (1991): Environmental Protection Agency, Office of Air Quality Planning and Standards, Research Triangle Park, NC.. Letter to Bart Croes, California Air Resources Board, May 18.

Bridier, I., H. Caralp, R. Loirat, B. Lesclaux and B. Veyret (1991): "Kinetic and Theoretical Studies of the Reactions of $CH_3C(O)O_2 + NO_2 + M <=> CH_3C(O)O_2NO_2 + M$ between 248 and 393 K and between 30 and 760 Torr," J. Phys. Chem. 95, 3594-3600.

Bufalini, J. J, T. A. Walter, and M. M. Bufalini (1977): Envrion. Sci. Technol. 11, 1181-1185.

Bufalini, J. J. and M. C. Dodge (1983): Environ. Sci. Technol. 17, 308-311.

Calvert, J. G., and J. N. Pitts, Jr. (1966): Photochemistry, John Wiley and Sons, New York.

Cantrell, C. A., J. A. Davidson, A. H. McDaniel, R. E. Shetter and J. G. Calvert (1990): "Temperature-Dependent Formaldehyde Cross Sections in the Near Ultraviolet Spectral Region," J. Phys. Chem. 94, 3902-3908.

CARB (1989): "Definition of A Low-Emission Motor Vehicle in Compliance with The Mandates of Health and Safety Code Section 39037.05 (Assembly Bill 234, Leonard, 1987)", Report by Mobile Sources Division, California Air Resources Board, El Monte, California. May 19.

CARB (1990): "Low-Emission Vehicles/Clean Fuels -- Technical Support Document," Mobile Source Division, Research Division, Stationary Source Division, and Technical Support Division, California Air Resources Board, Sacramento, CA.

CARB (1991): "Proposed Reactivity Adjustment Factors for Transitional Low-Emissions Vehicles: Technical Support Document," California Air Resources Board, Sacramento, CA., September 27.

Carter, W. P. L., R. Atkinson, A. M. Winer, and J. N. Pitts, Jr. (1982), "Experimental Investigation of Chamber-Dependent Radical Sources," Int. J. Chem. Kinet., 14, 1071.

Carter, W. P. L., and R. Atkinson (1985): "Atmospheric Chemistry of Alkanes", J. Atmos. Chem., 3, 377-405, 1985.

Carter, W. P. L., F. W. Lurmann, R. Atkinson, and A. C. Lloyd (1986a), "Development and Testing of a Surrogate Species Chemical Reaction Mechanism," EPA-600/3-86-031, August.

Carter, W. P. L. and R. Atkinson (1987): "An Experimental Study of Incremental Hydrocarbon Reactivity," Environ. Sci. Technol. 21, 670.

Carter, W. P. L. and R. Atkinson (1989a): "A Computer Modeling Study of Incremental Hydrocarbon Reactivity", Environ. Sci. and Technol., 23, 864.

Carter, W. P. L. and R. Atkinson (1989b): "Alkyl Nitrate Formation from the Atmospheric Photooxidation of Alkanes; a Revised Estimation Method," J. Atm. Chem. 8, 165-173.

Carter, W. P. L. (1989a): "Estimates of Photochemical Reactivities of Solvent Species Used in Architectural Coatings," presented at the 82nd Annual Meeting of the Air and Waste Management Association, Anaheim California, June 25-30.

Carter, W. P. L. (1989b): "Ozone Reactivity Analysis of Emissions from Motor Vehicles," Draft Report to the Western Liquid Gas Association, July.

Carter, W. P. L. (1990): "A Detailed Mechanism for the Gas-Phase Atmospheric Reactions of Organic Compounds," Atm. Environ., 24A, 481-518.

Carter, W. P. L., and F. W. Lurmann (1990): "Evaluation of the RADM Gas-Phase Chemical Mechanism," Final Report, EPA-600/3-90-001.

Carter, W. P. L. (1991): "Development of Ozone Reactivity Scales for Volatile Organic Compounds", EPA-600/3-91/050, August.

Carter, W. P. L. and F. W. Lurmann (1991): "Evaluation of a Detailed Gas-Phase Atmospheric Reaction Mechanism using Environmental Chamber Data," Atm. Environ. 25A, 2771-2806.

Carter, W. P. L., J. A. Pierce, I. L. Malkina, D. Luo, and W. D. Long (1993): "Environmental Chamber Studies of Maximum Incremental Reactivities of Volatile Organic Compounds," Report on Coordinating Research Council Project ME-9 and California Air Resources Board Contract No. A032-0692, April 1.

California Advisory Board on Air Quality and Fuels (1989): "Report to the California Legislature, Volume I – Executive Summary," Final Report to the California Air Resources Board, Contract No. A766-177, October 2.

Chameides, W. L., F Fehsenfeld, M. O. Rodgers, C. Cardelino, J. Martinez, D. Parrish, W. Lonneman, R. R. Lawson, R. A. Rasmussen, P. Zimmerman, J. Greenburg, P. Middleton, and T. Wang (1992): "Ozone Precursor Relationships in the Ambient Atmosphere," J. Geophys. Res. 97, 6037-6055.

Chang, T. Y. and S. J. Rudy (1990): "Ozone-Forming Potential of Organic Emissions from Alternative-Fueled Vehicles," Atmos. Environ., 24A, 2421-2430.

Croes, B. E. (1991): "Development and Evaluation of Ozone Reactivity Scale for Low-Emissions Vehicles and Clean Fuels Regulations," California Air Resources Board, Research Division, January 14, 1991.

Croes, B. E. (1991): Technical Support Division, California Air Resources Board, personal communication.

Croes, B. E., J. R. Holmes, and A. C. Lloyd (1992): "ARB/SCAQMD Conference on Reactivity-Based Hydrocarbon Controls: Scientific Issues and Potential Regulatory Applications", submitted to JAPCA

Croes., B. E. et al. (1993): "Southern California Air Quality Study Data Archive," California Air Resources Board, in preparation.

Darnall, K. R., A. C. Lloyd, A. M. Winer, J. N. Pitts, Jr. (1976): Environ. Sci. Technol. 10, 692.

Derwent, R. G. and Hov, Ö (1979): "Computer Modelling Studies of Photochemical Air Pollution Formation in North West Europe," AERE R 9434, Harwell Laboratory, Oxfordshire, England.

Derwent, R. G. and Hough, A. M. (1988): "The Impact of Possible Future Emission Control Regulations on Photochemical Ozone Formation in Europe," AERE R 12919, Harwell Laboratory, Oxfordshire, England.

Derwent, R. G. and M. E. Jenkins (1991): "Hydrocarbons and the Long Range Transport of Ozone and PAN over Europe," Atmos. Environ., 25A, 1661.

Dodge, M. C. (1977), "Combined Use of Modeling Techniques and Smog Chamber Data to Derive Ozone-Precursor Relationships" in Proc. International Conference on Photochemical Oxidant and Its Control, Research Triangle Park, North Carolina, EPA-600/3-80-028a.

Dodge, M. C. (1984): "Combined Effects of Organic Reactivity and NMHC/NOx Ratio on Photochemical Oxidant Formation -- A Modeling Study," Atmos. Environ., 18, 1657.

EPA (1984): "Guideline for Using the Carbon Bond Mechanism in City-Specific EKMA," EPA-450/4-84-005, February.

Gery, M. W., R. D. Edmond, and G. Z. Whitten (1987), "Tropospheric Ultraviolet Radiation. Assessment of Existing Data and Effects on Ozone Formation," Final Report, EPA-600/3-87-047, October.

Gery, M. W., G. Z. Whitten, and J. P. Killus (1988): "Development and Testing of the CBM-IV For Urban and Regional Modeling,", EPA-600/ 3-88-012, January.

Gery, M. W. (1991): "Review of the SAPRC-90 Chemical Mechanism," Final Report, California Air Resources Board Contract No. A132-055, August 8.

Gipson, G. L., W. P. Freas, R. A. Kelly, and E. L. Meyer (1981): "Guideline for Use of City-Specific EKMA in Preparing Ozone SIPs, EPA-450/4-80-027, March.

Gipson, G. L. and W. P. Freas (1983): "Use of City-Specific EKMA in the Ozone RIA", U. S. Environmental Protection Agency, July.

Gipson, G. L. (1984) "Users Manual for OZIPM-2: Ozone Isopleth Plotting With Optional Mechanisms/Version 2", EPA-450/4-84-024, August

Hough, A. M. and R. G. Derwent (1987): "Computer Modelling Studies of the Distribution of Photochemical Ozone Production Between Different Hydrocarbons," Atmos. Environ. 21, 2015-2033.

Hough, A. M. (1988), "An Intercomparison of Mechanism for the Production of Photochemical Oxidants," J. Geophys. Res., 93, 3789-3812.

Jeffries H. E., K. G. Sexton, J. R. Arnold, and T. L. Kale (1989): "Validation Testing of New Mechanisms with Outdoor Chamber Data. Volume 2: Analysis of VOC Data for the CB4 and CAL Photochemical Mechanisms," Final Report, EPA-600/3-89-010b.

Jeffries, H. E. and R. Crouse (1991): "Scientific and Technical Issues Related to the Application of Incremental Reactivity. Part II: Explaining Mechanism Differences," Report prepared for Western States Petroleum Association, Glendale, CA, October.

Jeffries, H. E. (1991), Department of Environmental Science and Engineering, School of Public Health, University of North Carolina, Chapel Hill, NC, private communication.

Joshi, S. B, M. C. Dodge, and J. J. Bufalini (1982): Atmos. Environ. 16, 1301-1310.

Laity, J. L., F. G. Burstain, and B. R. Appel (1973): "Photochemical Smog and The Atmospheric Reactions of Solvents," in "Solvents Theory and Practice," Tess, R. W., Ed., Adv. Chem. Series 124, 95.

Lowi, A. L., and W. P. L. Carter (1990): "A Method for Evaluating the Atmospheric Ozone Impact of Actual Vehicle Emissions," Presented at the SAE International Congress and Exposition, Detroit, Michigan, February 26 - March 2, 1990.

Lurmann, F. W., W. P. L. Carter, and R. A. Coyner (1987): "A Surrogate Species Chemical Reaction Mechanism for Urban-Scale Air Quality Simulation Models. Volume I - Adaptation of the Mechanism," EPA-600/3-87-014a.

Lurmann, F. W., H. H. Main, K. T. Knapp, L. Stockburger, R. A. Rasmussen and K. Fung (1992): "Analysis of the Ambient VOC Data Collected in the Southern California Air Quality Study," Final Report to California Air Resources Board Contract No. A832-130, February.

Rogers, J. D. (1990): "Ultraviolet Absorption Cross Sections and Atmospheric Photodissociation Rate Constants of Formaldehyde," J. Phys. Chem., 90, 4011-4015.

Russell, A, J. Harris, J. Milford, and D. St.Pierre (1989): "Quantitative Estimate of the Air Quality Impacts of Methanol Fuel Use," Final report, California Air Resources Board Agreement No. A6-048-32, Carnegie-Mellon University, Pittsburgh, PA, April.

Russell, A. G. (1990): "Air Quality Modeling of Alternative Fuel Use in Los Angeles, CA: Sensitivity of Pollutant Formation to Individual Pollutant Compounds," the AWMA 83rd Annual Meeting, June 24-29.

Stockwell, W. R., P. Middleton, J. S. Chang, and X. Tang (1990): "The Second Generation Regional Acid Deposition Model Chemical Mechanism for Regional Air Quality Modeling," J. Geophys. Res. 95, 16343- 16376.

Tuazon, E. C., W. P. L. Carter, R. Atkinson, and J. N. Pitts, Jr. (1983): Int. J. Chem. Kinet. 15, 619.

Tuazon, E. C., W. P. L. Carter and R. Atkinson (1991): "Thermal Decomposition of Peroxyacetyl Nitrate and Reactions of Acetyl Peroxy Radicals with NO and NO_2 Over the Temperature Range 283-313 K," J. Phys. Chem., in 95, 2434.

Weir, B. R., A. S. Rosenbaum, L. A. Gardner, G. Z. Whitten and W. Carter, (1988): "Architectural Coatings in the South Coast Air Basin: Survey, Reactivity, and Toxicity Evaluation", Final Report to the South Coast Management District, SYSAPP-88/137, Systems Applications, Inc. San Rafael, CA, December.

Wilson, K. W., and G. J. Doyle (1970): "Investigation of Photochemical Reactivities of Organic Solvents," Final Report, SRI Project PSU-8029, Stanford Research Institute, Irvine CA, September.